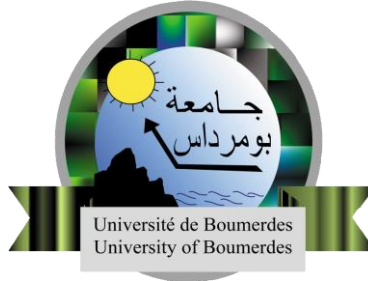**People's Democratic Republic of Algeria**
Ministry of Higher Education and Scientific Research

University M'Hamed BOUGARA – Boumerdes

Institute of Electrical and Electronic Engineering

Department of Power and Control

Final Year Project Report Presented in Partial Fulfilment of
the Requirements for the Degree of the

MASTER

In **Power Engineering**

Option: **Power Engineering**

Title:

Fuzzy Logic Based Energy Management for Standalone Hybrid Renewable Energy System

Presented by:

- **ZEMOURA Mohamed Taha**
- **KESSITA Yaakoub**

Supervisor:

Dr. AMMAR Abdelkarim

Registration Number:........./2023

Abstract

The increasing demand for sustainable and reliable energy sources has led to the emergence of hybrid renewable energy systems as viable alternatives in standalone applications. This report presents a comprehensive study on the design, modeling, control, and simulation of a hybrid renewable energy system consisting of a photovoltaic (PV) array integrated with a battery storage system and a backup diesel engine. A detailed matematical model is developed to capture the dynamic behavior of the PV array, battery storage system, and diesel engine, taking into account factors such as solar irradiance, battery state of charge, load demand, and diesel fuel consumption. The proposed control strategy utilizes a combination of power scheduling, load forecasting, and state-of-charge management techniques to ensure optimal operation and seamless transition between PV, battery, and diesel power sources, using Fuzzy Logic. The control algorithm is implemented and validated through simulation studies using advanced software tools, providing a realistic representation of the hybrid system's performance under various operating conditions and load profiles.

Dedication

This report is dedicated to my lovely parents and sisters for their endless love,support and encouragement. I further extend my dedication to all members of Kessita's family.

I would like to also extend my heartfelt dedication to all my friends and colleagues, and all the teachers and staff who helped me throughout this process.

Yaakoub

This report is dedicated to my lovely parents and Brother for their endless support and encouragement. I further extend my dedication to all members of Zemoura's family.

I would like to also extend my heartfelt dedication to all my friends, colleagues, and teachers who have been an invaluable support throughout my journey. Additionally, I wish to express my deepest gratitude to those who have taught, encouraged, and provided guidance to me throughout my entire academic pursuit. This master's report is dedicated to each and every one of them, with sincere appreciation and admiration.

Mohamed Taha

Acknowledgment

First and foremost, all praise and thanks giving to Allah the most powerful and most merciful who gave us the ability and patience to accomplish the work presented.

We would like to express our deepest gratitude to our supervisor, Dr. AMMAR Abdelkarim, for his valuable insights and continuous support throughout the research and writing process. Their expertise and encouragement have been instrumental in shaping this report.

This report was carried out in the electronics institute of the University of Boumerdes. We would like to express our sincere thanks to all the university staff who assisted us throughout our masters studies and offered us a very pleasant studying environment.

We would like to also express our gratitude to all the members of jury for their valuable time and feedback.

Contents

List of Figures

List of Tables

List of Abbreviations

HES Hybrid Energy System

HRES Hybrid Renewable Energy System

PV Photovoltaic

AC Alternating Current

DC Direct Current

DG Diesel Engine

VRLA Valve Regulated Lead Acid

NPC Net Present Cost

SOC State of Charge

DOD Depth of Discharge

PMSG Permanent Magnet Synchronous Generator

EMS Energy Management System

RBS Rule Based Strategies,

OBS Optimization Based Strategies

FBS Frequency Based Strategies

AI Artificial Intelligence

DS Deterministic Strategies

PHEVs Plug-in Hybrid Electric Vehicles

EVs Electrical Vehicles

LOS Local Optimization Strategies

GOS Global Optimization Strategies

SOH State of Health

VOC Voltage Oriented Control

PWM Pulse Width Modulation

General Introduction

The global energy landscape is currently experiencing a substantial transformation, driven by growing environmental concerns and the urgent need for sustainable power generation. This shift is motivated by several factors, including the recognition of the detrimental effects of traditional energy sources on the environment and the realization that a transition to renewable energy is vital for addressing climate change and achieving long-term sustainability.

The increasing concentration of greenhouse gases in the atmosphere, primarily caused by the combustion of fossil fuels, has resulted in a range of environmental issues such as global warming, air pollution, and ecosystem degradation. These concerns have triggered widespread calls for a transition towards cleaner and more sustainable energy sources that have minimal or no greenhouse gas emissions.

Renewable energy sources, such as solar, wind, hydroelectric, geothermal, and biomass, offer promising alternatives to traditional fossil fuel-based energy systems. They harness the power of naturally replenishing resources and have a significantly lower environmental impact compared to conventional energy sources. Renewable energy technologies have been rapidly advancing, becoming more efficient, cost-effective, and reliable, making them increasingly attractive for large-scale power generation. Hybrid Renewable Energy Systems (HRES) have emerged as a promising solution that integrates multiple renewable energy sources, such as photovoltaic (PV) systems, energy storage systems (e.g., lead-acid batteries), and backup diesel generators. This thesis focuses on fuzzy logic control-based energy management for a

hybrid renewable energy system consisting of PV, battery, and backup diesel components.

Chapter 1 provides an overview of HRES, discussing different types of configurations, including grid-connected systems, standalone systems, and hybrid systems. The components of our specific HRES, namely PV generators, lead-acid batteries, and a Permanent Magnet Synchronous Generator (PMSG) coupled with a diesel engine, are explained in detail. The advantages of HRES, such as reduced carbon emissions, increased energy independence, and improved system reliability, are discussed alongside the challenges faced in optimizing the utilization of renewable energy sources, efficient energy storage, and integration of backup power sources.

Chapter 2 focuses on the modeling of HRES components. These models capture the electrical, mathematical, and mechanical characteristics of each component, enabling accurate representation and performance evaluation.

Chapter 3 delves into the control strategies for different HRES components. Maximum Power Point Tracking (MPPT) control algorithms are designed and implemented for the PV system, optimizing power generation under varying environmental conditions. PI (Proportional-Integral) controllers are employed for efficient battery management, regulating charging and discharging processes. Fuzzy Logic Control (FLC) is utilized for energy management, intelligently coordinating the power flow between the PV system, battery, and backup diesel generator, considering factors such as renewable energy availability, load demand, and system constraints.

Chapter 4 presents simulation results and discussion. The different scenarios used to evaluate the HRES and its energy management system. The performance of components and overall system is assessed in terms of Power flow and stability. The analysis is conducted to evaluate the effectiveness of the fuzzy logic control in the proposed system

In summary, this report focuses on fuzzy logic control-based energy management for

a hybrid renewable energy system comprising PV, battery, and backup diesel generator. It provides an overview of HRES, discusses system components, advantages, and challenges, presents modeling techniques, control strategies, and simulation results. The goal is to optimize energy utilization, improve system performance, and promote the integration of renewable energy sources into the power generation mix.

Chapter1

Overview on Hybrid renewable energy systems and Energy Management

Chapter 1

Overview on Hybrid renewable energy systems and Energy Management

1.1 Introduction

This Chapter emphasizes the importance of HRES in sustainable energy generation and explores its potential benefits and addresses the challenges associated with HRES implementation. This chapter further discusses the key components of HRES, including renewable energy generators, energy storage systems, back up generators. Lastly, it explores various energy management strategies to optimize system performance and maximize economic benefits.

1.2 Hybrid Energy Systems

Hybrid energy systems involve the combination of two or more energy conversion devices or fuels to overcome any constraints that may arise when using them individually. This definition is beneficial as it encompasses a wide range of scenarios and emphasizes the importance of having diverse energy conversion options. It should

be noted that this broad definition allows for the inclusion of transportation energy systems and does not mandate that a device be exclusively powered by renewable energy, typically, a hybrid energy system consists of a primary energy source, which is often a renewable energy source like solar, wind, or hydro, and a secondary energy source, which is usually a conventional energy source like fossil fuels or a storage system such as batteries or fuel cells.

The primary energy source provides the bulk of the power generation, while the secondary source acts as a backup or supplement during periods of low renewable energy availability or increased demand.The components of a hybrid energy system may include renewable energy generators (such as solar panels, wind turbines, or hydroelectric generators), energy storage systems (like batteries or pumped hydro storage), conventional generators (such as diesel generators or natural gas turbines), power conversion and control devices, and a smart control system to manage and optimize the energy flow between the different sources[1].

1.3   HRES Based on Grid connection

1.3.1   Grid-Connected Hybrid Systems

An energy system that is connected to a grid (Figure 1), and operates independently is referred to as a grid-connected energy system. These systems are well-suited for areas located in close proximity to the grid. The functionality of a grid-connected energy system relies on the availability of supply sources. It operates only when the supply sources are accessible. In situations where there is a shortage of supply sources, the system may need to prioritize the overall supply rather than local demand due to its supply-driven operation.

In a grid-connected power system, the grid acts like an infinitely large battery. It effectively accommodates fluctuations in seasonal load. Consequently, a grid-connected system tends to be more efficient compared to a stand-alone system. The storage capacity is virtually unlimited, allowing generated electricity to be stored,
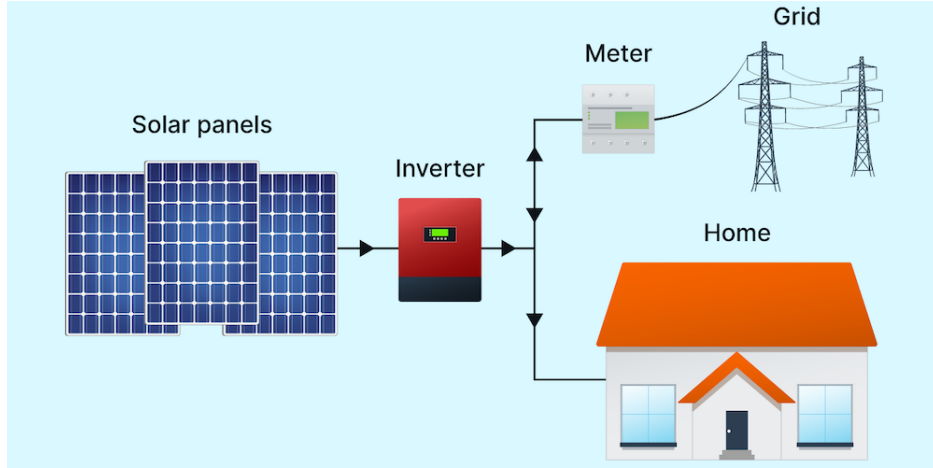
Figure 1: Grid connected hybrid system.

and any excess electricity produced does not go to waste.

Apart from the initial purchase price of the system, there are additional costs associated with the grid interface of the system. These costs need to be taken into consideration. Considering that grid-connected systems often operate on a larger scale and require a substantial amount of biomass for their operation, there is a significant demand for renewable sources such as biomass, wind, and solar PV.[2]

1.3.2   Grid-Isolated Hybrid Systems

Stand-alone systems, also known as off-grid systems as shown in Figure 2, are characterized by their ability to operate independently of the utility grid as they generate their own electricity. These systems are particularly suitable for extremely remote areas where grid access is unavailable and alternative energy sources are scarce. These systems often present the most cost-effective solution for applications situated far from the utility grid, making them prevalent in solar installations across remote regions worldwide. They find application in various scenarios, including emergency services or military use, lighthouses, other remote locations, and facilities involved in the manufacturing of sensitive electronics.

They are disconnected from the utility grid, they require additional batteries and storage devices to store the generated electricity during periods of low demand.
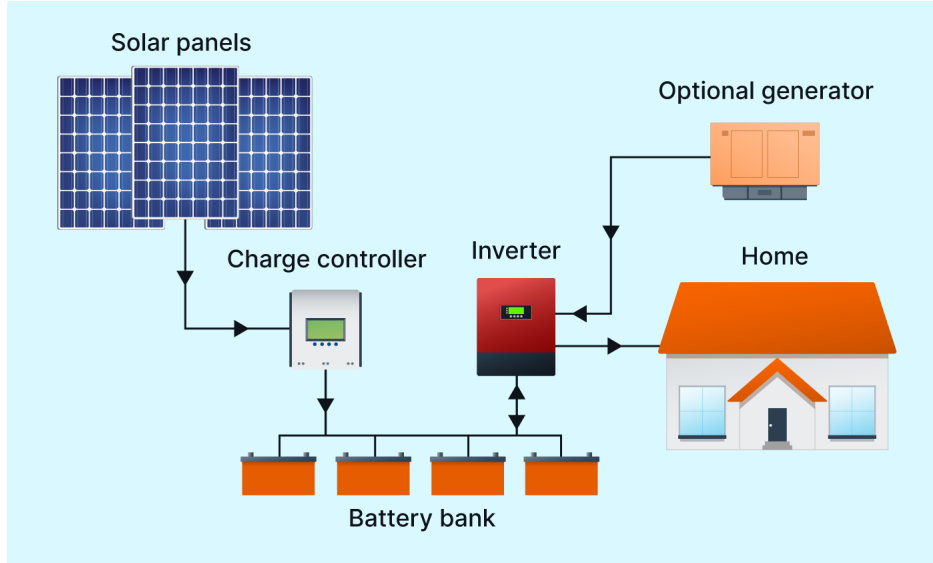
Figure 2: Grid isolated hybrid system.

Otherwise, any excess power produced would be wasted and unused. This necessity arises due to the absence of a grid connection, necessitating the careful management and storage of surplus energy to meet power demands during times of limited or no generation.[2]

1.3.3   Hybrid solar systems

Hybrid solar systems as shown in Figure 3, combine the best features of grid-tied and off-grid solar systems, offering enhanced flexibility and reliability. These systems can be described as either off-grid solar systems with utility backup power or grid-tied solar systems with additional battery storage.

In the case of grid-tied solar systems, if you also own an electric vehicle (EV) that runs on electricity, you already have a hybrid setup to some extent. This is because an EV essentially functions as a battery on wheels. The EV's battery can store electricity generated by the grid-tied solar system and utilize it to power the vehicle. Conversely, during times when the solar system produces excess electricity, it can be directed towards charging the EV's battery.

This hybrid configuration allows for increased self-consumption of solar energy, reducing reliance on the grid and optimizing the use of renewable energy. It provides
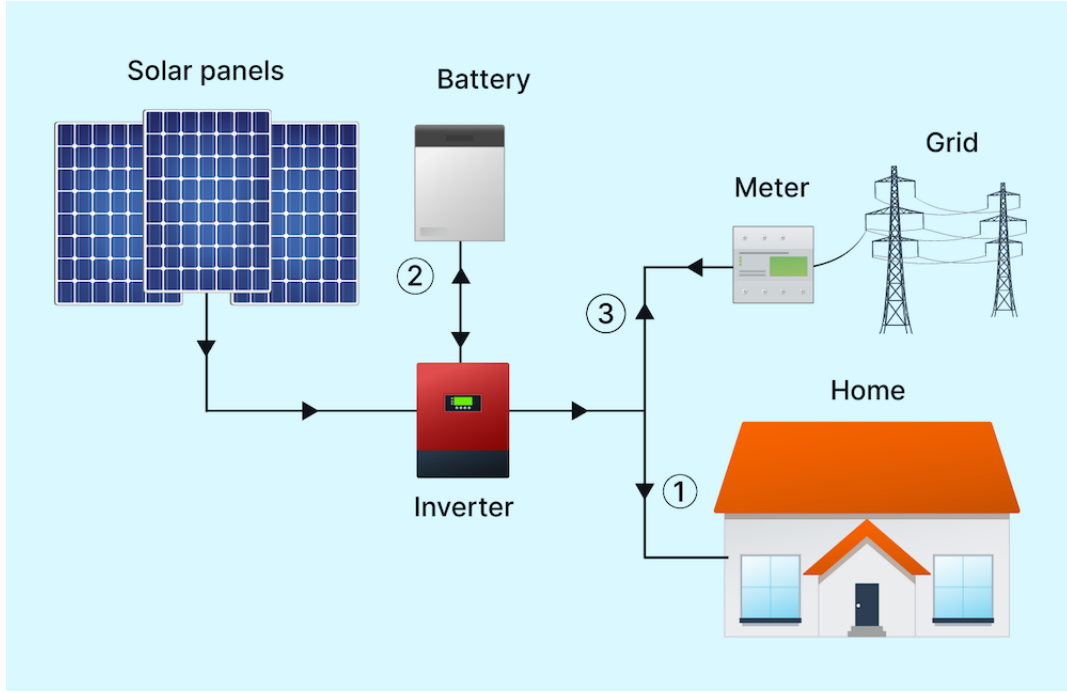
Figure 3: Hybrid solar system.

the advantage of using clean solar power to charge the EV, reducing carbon emissions associated with traditional fossil fuel vehicles.

By combining a grid-tied solar system with an electric vehicle, you are effectively integrating two sustainable technologies, maximizing the benefits of both and moving towards a more environmentally friendly and energy-efficient lifestyle[3].

1.4 Applications for Hybrid Energy Systems

Hybrid power systems offer a wide range of potential applications, with typical examples including isolated or specialized electrical loads, distributed generation in traditional utility networks, and remote AC networks.

A common example of a hybrid energy system is a remote AC network powered by diesel. The primary goal of such a system is to reduce fuel consumption and operating hours of diesel generators. To achieve this, the first step is to introduce a different type of generator, often one that utilizes a renewable resource such as solar or wind turbines. However, experience has shown that simply adding a second

generator is not sufficient to achieve the desired outcomes.

Therefore, most hybrid systems incorporate additional features such as load management, short-term energy storage, and supervisory control systems to optimize performance. Each of these components plays a crucial role in the overall design. Figure 4. provides an illustration of a typical hybrid energy system, specifically a solar battery system with diesel engine backup.
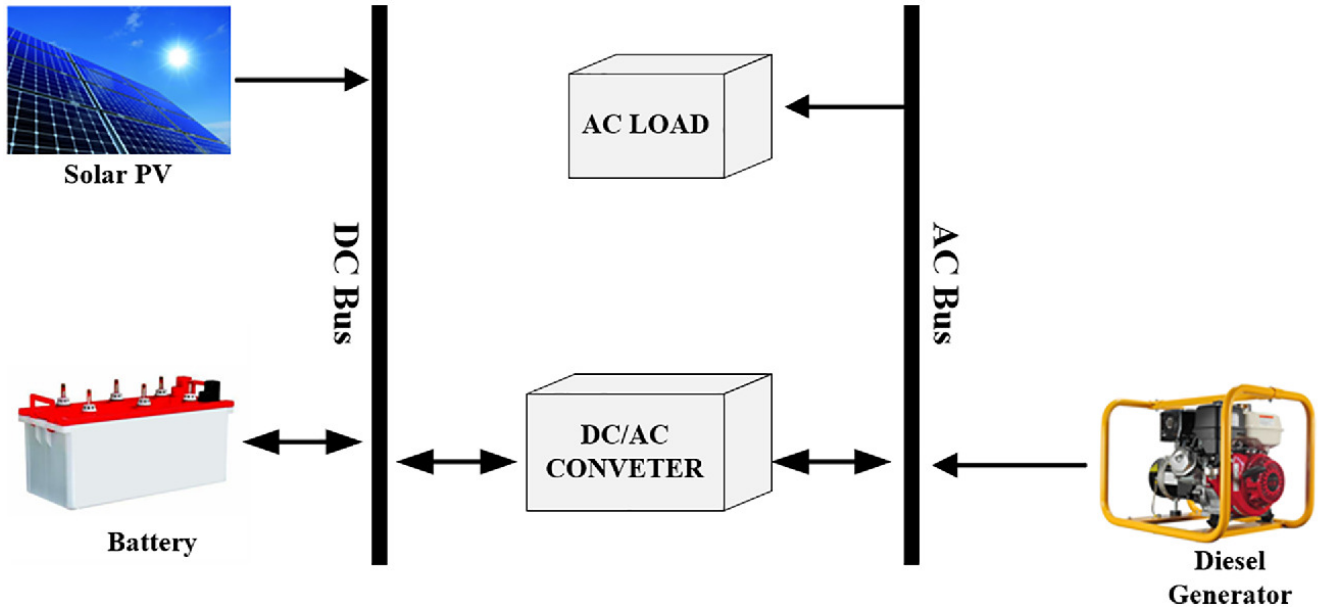
Figure 4: HES of PV/Battery with Diesel backup

With the management changes in many large electrical networks during the 1990s, individuals or organizations now have the opportunity to add generation capacity to the distribution systems operated by utility companies. This concept is referred to as distributed generation (DG). By combining the distributed generator with various energy conversion devices, diversified production can serve a range of purposes, resulting in a hybrid energy system.

Hybrid systems prove particularly valuable when employed in conjunction with isolated or specialized applications. For instance, solar panels, battery storage, and power electronic converters can be utilized to provide a small amount of energy to a load in a remote area. Water pumping and desalination are other examples where hybrid systems can be deployed. In these applications, electrical loads can vary in

terms of voltage, frequency, and whether they are AC or DC-powered.[1]

1.5   Advantages and Challenges of HES

Hybrid energy systems offer numerous advantages in the field of energy production. One key benefit is their ability to harness the complementary nature of various energy sources. By combining different sources, these systems can increase reliability and efficiency. In particular, hybrid solar energy systems are known for their superior performance compared to traditional generators, as they operate more efficiently and sustainably, minimizing fuel waste.

Another advantage of hybrid energy systems is their long-term cost-effectiveness. While the initial investment may be high, these systems eliminate the need for fuel, unlike traditional generators, resulting in significant savings over time. Additionally, hybrid systems require less frequent maintenance, further reducing expenses, furthermore, hybrid energy systems play a crucial role in promoting renewable energy. By integrating renewable sources, such as solar and wind power, hybrid systems help reduce reliance on fossil fuels and contribute to a cleaner and more sustainable energy mix[4].

Despite their benefits, hybrid energy systems also face certain challenges. Improving system efficiency and extending the lifespan of the engine requires further research and development. Condition monitoring and power distribution management pose critical difficulties in hybrid systems, demanding effective strategies for their operation[5].

Moreover, policy considerations play a significant role in the implementation of hybrid energy systems. The hybridization of energy sources presents opportunities and challenges for designing, operating, and regulating energy markets and policies. This may necessitate adjustments to existing processes, such as permitting, siting, interconnection, and policy implementation, to accommodate hybrid systems effectively[6].

1.6 Hybrid Sytstem's Components

This section will provide a quick overview of the main elements comprising our hybrid energy system. It is important to discuss these elements in more detail in the next chapter. The descriptions provided here will serve as a brief introduction, with a focus on highlighting the main components of our hybrid energy system. This section introduce the three main components of our hybrid energy system.[1]:

1.6.1 Photovoltaic Panels

Solar energy is harnessed as a renewable source to generate electricity using photovoltaic (PV) panels. These panels consist of multiple individual cells that are interconnected to produce power at a specific voltage. It is important to note that photovoltaic panels inherently operate on direct current (DC), necessitating the use of an inverter to convert the generated electricity into alternating current (AC).
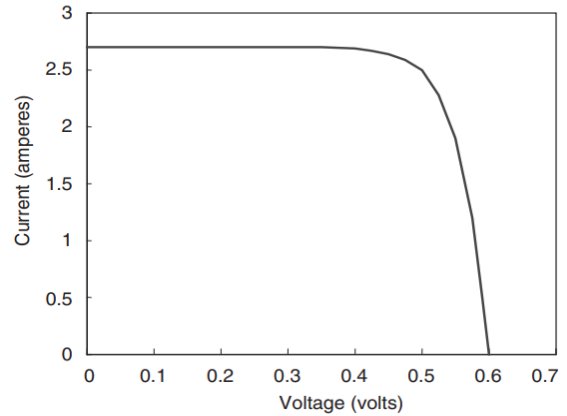
Figure 5: PV panel with its current versus voltage curve.

The primary component of PV cells is crystalline silicon, which serves as the main material for their construction. The performance of PV cells is directly influenced by solar energy, with the current produced by the cells being proportionate to the amount of solar radiation received. Figure 5 provides a visualization of the PV pannel and its current/voltage relationship exhibited by a typical silicon cell under constant solar radiation. It is noteworthy that the power output of a PV cell con-

tinues to rise until the current begins to decrease, as power is determined by the product of current and voltage.

To accommodate the voltage requirements, PV panels are configured with multiple cells connected in series. This arrangement is necessary because the maximum voltage produced by each individual cell is typically less than 1 V. By connecting cells in series, the overall voltage output of the PV panel can be increased to meet the desired specifications.

Considering the dynamic nature of solar radiation, it is essential to acknowledge that the actual radiation levels experienced at a specific location on Earth's surface can significantly vary over the course of a year and within a single day.

1.6.2 Energy Storage System

Batteries are the most widely used type of energy storage in hybrid energy systems, offering the flexibility of both short-term (less than an hour) and long-term (more than a day) storage. In standalone systems, various types of batteries can be uti-

Table 1.1: Comparison of Lead Acid Batteries and Lithium-ion Batteries for Standalone Power Systems

Factors	Lead Acid Batteries	Lithium-ion Batteries
Cost-effectiveness	Relatively inexpensive	Higher cost, but decreasing
Durability	Robust and can withstand harsh conditions	Sensitive to high temperatures and require thermal management
Deep Discharge	Can handle deep discharge cycles	Not recommended for deep discharge
Availability	Widely available	Growing availability
Maintenance	Requires periodic maintenance	Minimal maintenance required
Energy Density	Lower energy density	Higher energy density
Lifespan	Shorter lifespan compared to lithium-ion batteries	Longer lifespan
Environmental Impact	Requires proper disposal due to lead content	More environmentally friendly and recyclable

lized. Lead-acid batteries, specifically valve-regulated lead-acid (VRLA) batteries,

are widely used in off-grid photovoltaic applications due to their cost-effectiveness for large capacities. However, lead-acid batteries have inherent weaknesses in PV systems and are being gradually replaced by newer technologies like lithium-ion (Li-ion) batteries. Despite their higher cost, Li-ion batteries can offer competitive advantages in certain cases, primarily due to their longer cycle life.

Estimating battery life accurately is crucial in the optimization process of standalone systems since the total battery cost, including replacements, significantly contributes to the system's net present cost (NPC). Errors in predicting battery lifetime can lead to substantial inaccuracies in estimating the NPC. Following table shows why lead acid batteries are used in this system :

The aging factors of lead-acid batteries include charge and discharge rates, charge throughput (Ah), time between full charges, time at a low state of charge (SOC), and partial cycling. Researchers have extensively analyzed these aging factors. Classical models commonly employed by researchers and software tools to estimate battery life are the "equivalent full cycles model" and the "rainflow cycle counting model."

The equivalent full cycles model quantifies the total charge (Ah throughput) cycled by the battery since its inception, disregarding variables such as SOC, temperature, and current. When this value reaches the manufacturer's specified cycle life obtained from standard tests, the battery is considered to have reached the end of its life. The rain flow cycle count model takes into account the depth of discharge (DOD). However, real operating conditions differ from laboratory conditions, including current rate, temperature, DOD, SOC, etc[7].

1.6.3 Diesel Engine/Generators

In a standalone power system, the PMSG (Permanent Magnet Synchronous Generator) combined with a diesel engine as shown in Figure 6, serves as a reliable backup power source. This backup system ensures a continuous supply of electrical power when the primary power sources, such as PV panels and battery banks, are unable

to meet the demand or encounter limitations.

When triggered, the backup power system activates the diesel engine, which starts and provides rotational mechanical energy. The PMSG, coupled with the diesel engine, plays a crucial role in converting this mechanical energy into usable electrical power. As the diesel engine rotates, the permanent magnets within the PMSG create a magnetic field. This magnetic field induces a voltage in the stator windings, resulting in the generation of electrical power. The output generated by the PMSG is typically in the form of alternating current (AC). To ensure the compatibility and
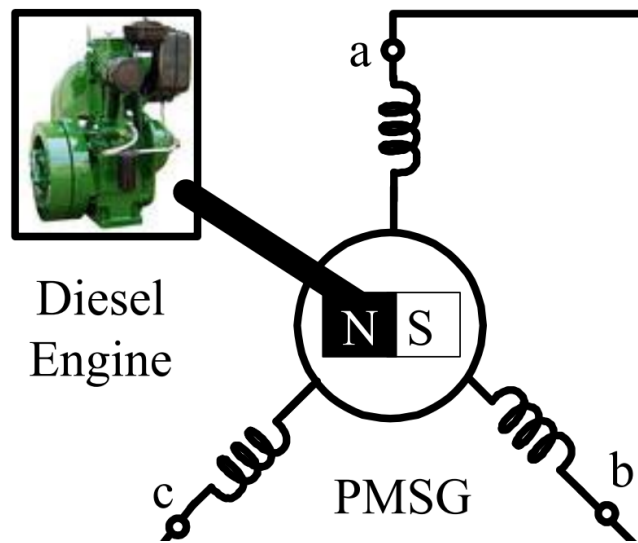

Figure 6: Diesel gen-set.

quality of the electrical power produced, the AC output from the PMSG often undergoes power conditioning. Power conditioning involves regulating and controlling various electrical parameters, such as voltage, frequency, and waveform shape. This process helps to stabilize and refine the electrical power generated by the PMSG, making it suitable for distribution and utilization in the standalone power system.

Once the electrical power from the PMSG is conditioned, it is distributed to the load or connected electrical systems within the standalone system. This distribution process typically involves the use of a distribution panel or an electrical grid, which ensures that the power reaches the intended destinations reliably and efficiently.

As the primary power sources, such as the PV panels and battery banks, regain

their capability to meet the electricity demand, the backup power system can be deactivated. The system transitions seamlessly back to the primary power sources for normal operation. This switch is often facilitated by a system controller or an automatic transfer switch, ensuring a smooth and uninterrupted transition.

By incorporating a PMSG with a diesel engine backup, the standalone power system gains enhanced resilience and reliability. This backup power source ensures a continuous supply of electricity during periods of high demand, extended periods of low sunlight, or when the battery bank charge level is low. It serves as a valuable safeguard, providing assurance that the power system can meet critical energy needs even under challenging circumstances[8].

1.7 Energy Management

1.7.1 Definition

The phrase energy management means different things to different people. To us, energy management is: The judicious and effective use of energy to maximize profits (minimize costs) and enhance competitive positions. This relatively broad description encompasses a variety of tasks, from the design of goods and machinery to their distribution. Numerous opportunities for energy management are also presented by waste reduction and disposal.

It is essential to approach energy management from a total systems perspective in order to assess and optimize a number of crucial processes.

Maximizing revenues or reducing costs is the main goal of energy management. The following are some desirable sub-objectives of energy management programs[9]:

1. Increasing energy efficiency and lowering energy consumption to cut costs.

2. Fostering effective communication on energy-related issues.

3. Creating and maintaining efficient management, monitoring, and reporting

plans for responsible energy use.

4. Discovering fresh and improved ways to boost energy investment returns through research and development.

5. Getting all staff to care about and commit to the energy management program.

6. Mitigating the effects of brownouts, blackouts, or any other interruptions in the energy supply.

1.7.2 Energy Management Strategies

An effective energy management strategy plays a crucial role in maximizing the performance of a system. It achieves this by reducing operating costs, prolonging the lifespan of storage components, meeting the immediate power demand of the system.
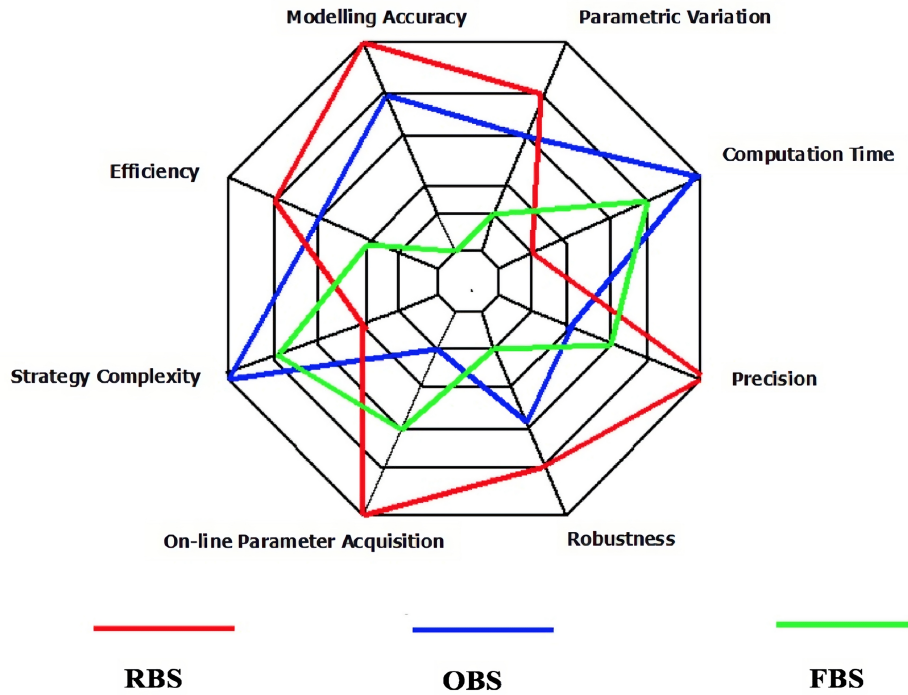

Figure 7: Energy management characteristics

In the literature, various energy management methods have been extensively studied, and they can be classified into three main categories: rule-based strategies (RBS), frequency-based strategies (FBS), and optimization-based strategies (OBS). Each

category exhibits distinct characteristics, as illustrated in Figure 7[10].

Rule Based Strategies(RBS)

Rule-based strategies (RBS) can further be categorized into deterministic strategies (DS) and artificial intelligence-based strategies (AI). DS involves the creation of strategies based on human intelligence, typically without prior knowledge of the driving cycle. On the other hand, AI algorithms are employed in AI-based strategies to analyze data, make predictions, and dynamically adjust to real-time conditions. Various artificial intelligence techniques, such as fuzzy logic, have been utilized in the development of these strategies.

RBS methods have found applications in controlling energy in various systems, including hybrid and plug-in hybrid electric vehicles (PHEVs). These strategies employ a set of predefined rules to determine the distribution and control of energy within the system.

In the context of PHEVs, the RBS approach involves limiting the engine power and allocating the remaining energy to the battery. For hybrid vehicles, the strategy focuses on dividing the power demand between the engine and the battery in a manner that ensures high efficiency of these power sources. These decisions are made based on human intelligence, intuitions, or mathematical models, often without prior knowledge of a specific drive cycle.

Overall, RBS is an easily implementable technique that utilizes a set of established rules to allocate and manage energy within a system. It can be applied to various systems, including hybrid vehicles, providing a practical approach for energy control and optimization.[11][12]

Frequency Based Strategies(FBS)

Frequency-based strategies (FBS) have been implemented in various systems, including hybrid electric vehicles, fuel cell electric vehicles, and stand-alone systems

with distributed battery storage. These strategies are particularly useful in managing the rapid power fluctuations in electric vehicles (EVs) due to the limitations of battery response time.

The aim of FBS is to separate the low frequency power, which can be effectively handled by batteries, from the high frequency power requirements in EVs. As batteries have slower dynamics, they are better suited for managing low frequency power demands.

In FBS systems, high frequencies are directed to one energy source, while low frequencies are routed to another source. This approach has been proposed and implemented in different systems, including fuel cell electric vehicles, stand-alone systems with dispersed battery storage, and hybrid electric vehicles. By effectively dividing the power based on frequency, FBS strategies help optimize the performance and efficiency of these systems.

Overall, FBS strategies play a crucial role in managing power fluctuations in EVs, leveraging the strengths of batteries and other energy sources to ensure a smooth and efficient operation. These strategies have wide-ranging applications in various energy systems, contributing to the advancement of sustainable transportation and distributed energy storage solutions[10].

Optimization Based Strategies(OBS)

Optimization-based energy management (OBS) refers to the application of mathematical optimization techniques to determine the most efficient and cost-effective methods of energy consumption. By formulating an optimization problem that considers multiple objectives, constraints, and energy-related factors, the optimal energy management strategy can be identified.

OBS can be further categorized into two main types: local optimization strategies (LOS) and global optimization strategies (GOS). LOS, also known as real-time optimization strategies, focuses on optimizing energy consumption in the immediate

context. These strategies aim to minimize an objective function in real-time, considering current system conditions and constraints.

On the other hand, GOS, also referred to as offline optimization strategies, take a broader view and aim to optimize energy consumption over a longer time horizon. These strategies consider the cumulative impact of energy usage by minimizing the sum of objective functions over time. GOS often involve analyzing historical data, forecasting energy demands, and making decisions that optimize energy efficiency and overall system performance.

The growing interest in OBS stems from its potential to achieve optimal outcomes in energy management. By employing mathematical optimization methods, OBS research endeavors to identify the most effective energy consumption patterns. This can lead to improved energy efficiency, cost savings, and environmental benefits.

Through the application of OBS, decision-makers can make informed choices about energy utilization, considering various factors such as energy demand, system constraints, and economic considerations. By optimizing energy management, OBS contributes to sustainable energy practices and the efficient use of resources[10].

1.7.3 EMS in Standalone

An Energy Management System (EMS) offers numerous benefits in standalone PV battery diesel systems. Here are the expanded benefits:

Fuel saving: An EMS plays a crucial role in fuel-saving applications within isolated hybrid systems, which combine solar, diesel, and battery sources. It optimizes the energy flow between these sources to minimize the operation of diesel generators and reduce fuel consumption[13].

Fulfillment of load demand: An efficient EMS ensures that the load demand is met effectively, providing stable operation by managing and balancing the power output from the PV system, battery storage, and diesel generators. It intelligently

controls the power flow to meet the required load while avoiding system overloads or underutilization[14].

Optimization of energy storage: An EMS actively monitors and optimizes the charging and discharging of the battery system. By analyzing the system's State of Charge (SOC) or State of Health (SOH), it determines the optimal input signal to charge or discharge the batteries. This maximizes the efficiency and lifespan of the battery storage, ensuring its optimal use.

Balancing multiple generation resources: Acting as an overall energy management system, an EMS ensures the seamless integration and coordination of multiple generation resources in line with grid requirements. It optimizes the utilization of solar power, battery storage, and diesel generators, dynamically adjusting their contribution based on the demand and availability of each source[15].

Achieving efficiency: One of the key capabilities of an EMS is to enable optimal and safe operation of standalone PV battery diesel systems. It continuously monitors and adjusts the energy flow, ensuring efficient utilization of available resources while maintaining system stability and reliability.

In summary, an EMS offers significant advantages in standalone PV battery diesel systems. It optimizes the efficiency, economy, and reliability of the system by reducing fuel consumption, fulfilling load demands, optimizing energy storage, balancing multiple generation resources, and ensuring efficient operation.

1.8   Conclusion

Chapter One provided a comprehensive overview of hybrid energy systems, including their definition, classification based on grid connection, advantages, and challenges. The components of our specific system, such as the PV system, battery storage system, and diesel engine, were discussed in detail, highlighting their roles and significance. Additionally, energy management and its various strategies, along with

their advantages, were explored. This knowledge forms the foundation for the subsequent chapters, enabling us to design, optimize, and evaluate our hybrid energy system for enhanced efficiency and sustainability.

Chapter2

System's Description and Configuration

Chapter 2

System's Description and Configuration

2.1 Introduction

Modeling the components of a hybrid energy system is a fundamental step in evaluating and comprehending their performance in various scenarios.

Through the development of precise models for each component, we can simulate their behavior, interactions, and overall operation within the system. This allows us to assess the system's efficiency, reliability, and feasibility before implementing it in practical applications. Our system configuration is shown in Figure 8. The modeling process of hybrid energy system components entails constructing mathematical representations or simulations that accurately depict their unique characteristics, dynamics, and responses to different inputs. By considering the following components of our hybrid energy system, a specific modeling can be considered .
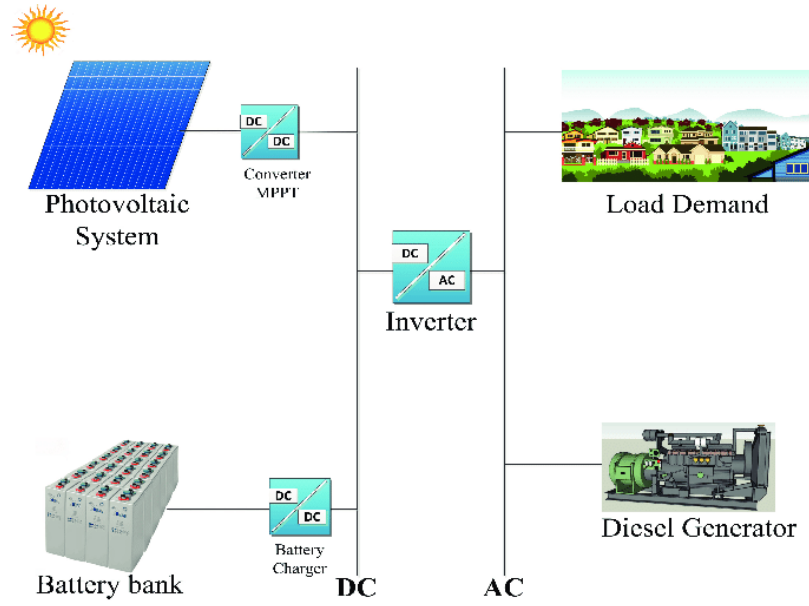
Figure 8: System's Configuration.

2.2 Modeling of the PV Generator

A photovoltaic system harnesses the energy from sunlight and transforms it into electrical energy. At the core of this system lies the photovoltaic cell, which alone generates a relatively small current or voltage, insufficient for most practical uses. Figure 9 provides a visual representation of a PV cell, module, array, and generator, illustrating their arrangement.
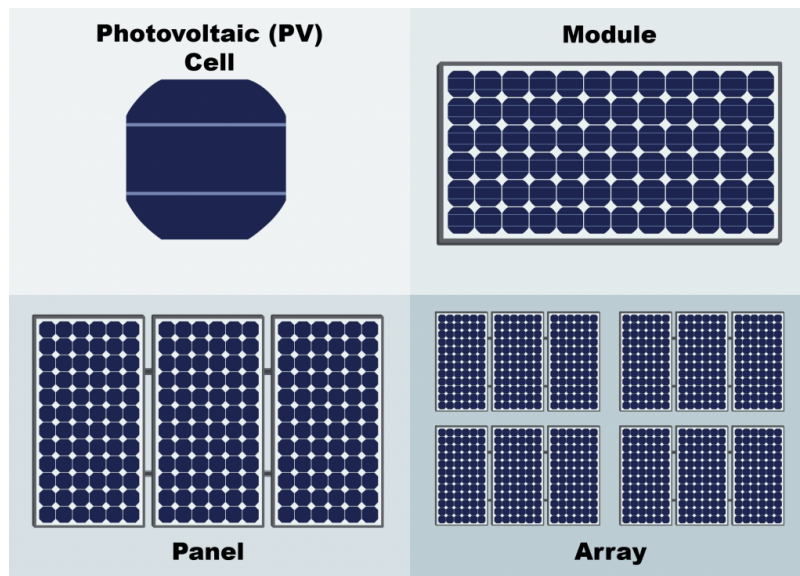

Figure 9: Illustration of PV cell, module, array, and generator.

To overcome this limitation, multiple cells are combined in series or parallel arrangements and then encapsulated within aluminum or glass structures to form solar modules.

These modules exhibit varying levels of current, voltage, and power output. The term "array" is commonly used to refer to a photovoltaic panel comprising multiple interconnected modules.

2.2.1 PV cell model

Under standard test conditions (1000W/m^2, 25°C), a silicon cell with an area of 150 cm^2 can generate a maximum power output of approximately 2.3W, accompanied by a voltage of 0.5V. Consequently, a single photovoltaic cell, in its basic form, acts as a low-power generator, rendering it inadequate for meeting the energy demands of most residential or industrial applications[16].
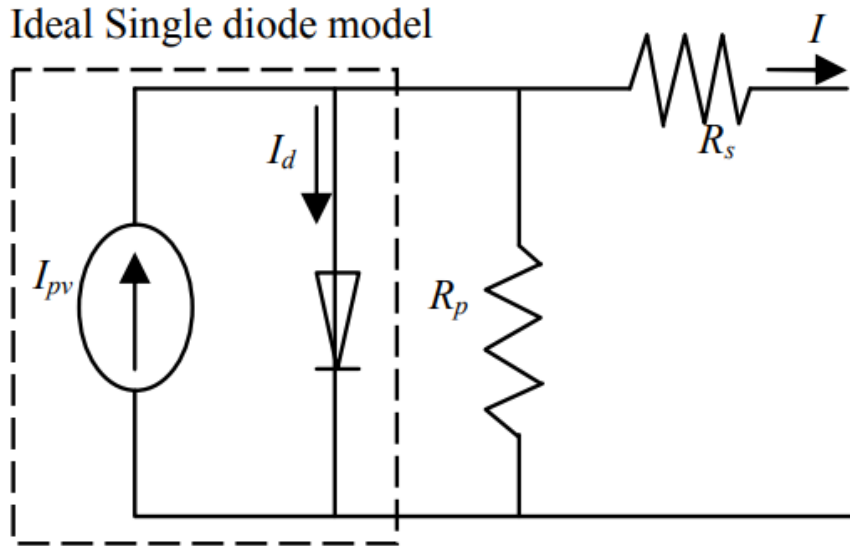

Figure 10: Single diode model.

The developed model incorporates fundamental circuit equations of Photovoltaic (PV) solar cells, taking into account the impact of solar irradiation and temperature fluctuations. By generating current in the presence of illumination and acting

as a diode in the absence of light, a PV cell can be represented by a current source connected in parallel with a diode[17]. The equivalent circuit model further includes internal resistances, represented by resistors Rs and Rsh, along with a shunt component. This configuration is depicted in the Figure 10.

The solar cell's physical structure resembles that of a diode, with the p-n junction exposed to sunlight. The underlying principles of semiconductor behavior can be described by the following equations:

$$I = I_{ph} - I_o \cdot \exp\left[\frac{q(V + IR_s)}{AKT_c} - 1\right] - \frac{V + IR_s}{R_{sh}} \tag{2.1}$$

$$V = \frac{AKT_c}{q} \ln\left[\frac{I_{ph} + I_o - I}{I_o}\right] - IR_s \tag{2.2}$$

Equation 2.1 can be written as :

$$I = I_{ph} - I_o \cdot \exp\left[\left(\frac{V + IR_s}{AV_t}\right) - 1\right] - \frac{V + IR_s}{R_s} \tag{2.3}$$

$$V_t = \frac{N_s KT_c}{q} \tag{2.4}$$

where:

- I: Cell output current in Amps

- I_{ph}: The Photocurrent, is the current produced by the incident light and function of irradiation level and junction temperature in Amps

- I_D: The diode current modeled by the equation for a Shockley diode in Amps

- I_o: The saturated reverse current or leakage current in Amps

- q: Electron charge (1.602×10^{-19} C).

- K: Boltzmann constant (1.38×10^{-23} J/°K)

- V: Cell output voltage, (V)

- T_0: Cell operating temperature, °K

- A: The diode ideality factor

- $R_{s,cell}$: Series resistance of the cell, Ohm

- $R_{sh,cell}$: Shunt resistance of the cell, Ohm

- V_t: Thermal voltage, V

- N_s: Number of series cells

2.2.2 Solar module model

To increase the total voltage of the module, cells have to be connected in series as shown in Figure 11 (a), ($V_{out} = V_1 + V_2 + V_3 + \ldots$).
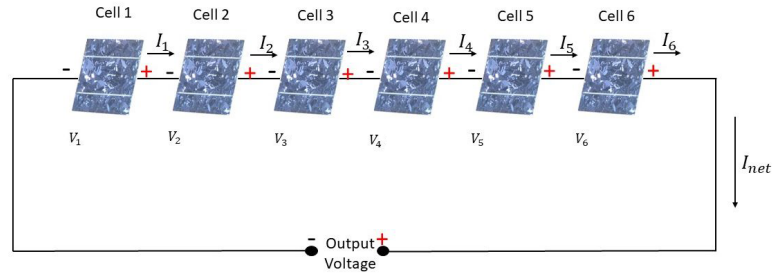
(a) Connecting PV cells in series
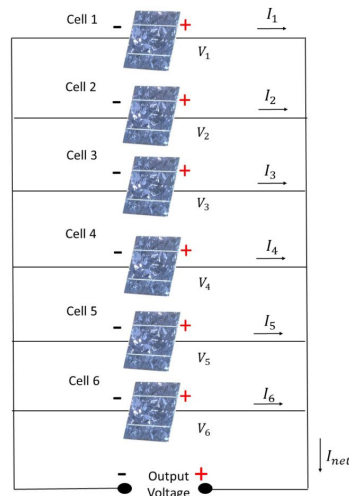
(b) Connecting PV cells in parallel.

Figure 11: Connecting PV cells in (a) series and (b) in parallel.

Connecting PV cells in parallel as shown in Figure 11 (b), increases the total current generated by the module ($I_{out} = I_1 + I_2 + I_3 + \ldots$).

When Np cells are connected in parallel branches and Ns cells are connected in series, the combined shunt resistance (Rsh Module) and series resistance (Rs Module) in the module are equal to:

$$R_{sh,module} = \left(\frac{N_p}{N_s}\right) \cdot R_{sh,cell} \tag{2.5}$$

$$R_{s,module} = \left(\frac{N_s}{N_p}\right) \cdot R_{s,cell} \tag{2.6}$$

where :

- $R_{sh,module}$: Total shunt resistance in the photovoltaic module, Ohm.

- $R_{s,module}$: Total series resistance in the photovoltaic module, Ohm.

- $R_{sh,cell}$: Shunt resistance in one photovoltaic cell, Ohm.

- $R_{s,cell}$: Series resistance in one photovoltaic cell, Ohm.

- N_s: Number of cells in series.

- N_p: Number of cell branches in parallel.

Then, the module current has an implicit expression depending on the following variables expressed in function of a single cell parameters and this is the approximation method[18]:

$$I_{sc,module} = N_p \cdot I_{sc,cell} \tag{2.7}$$

$$V_{oc,module} = N_s \cdot V_{oc,cell} \tag{2.8}$$

where:

- Isc,module: Total short circuit current of the photovoltaic module, measured in Amperes (A).

- Voc,module: Total open circuit voltage of the photovoltaic module, measured

in Volts (V).

- Isc,cell: Short circuit current of one photovoltaic cell, measured in Amperes (A).

- Voc,cell: Open circuit voltage of one photovoltaic cell, measured in Volts (V).

2.2.3 Solar array model

The PV system usually includes interconnected modules arranged in arrays. Figure 12 demonstrates an example of an array consisting of Mp parallel branches, each containing Ms modules connected in series. The voltage applied at the terminals of the array is represented by Varray, while the overall current of the array is denoted by:

$$I_{array} = \sum_{i=0}^{Mp} I_i \qquad (2.9)$$

Under the assumption that the modules are identical and the ambient irradiation is uniform across all modules, the current of the array can be expressed as:

$$I_{array} = M_p \cdot I_M \qquad (2.10)$$
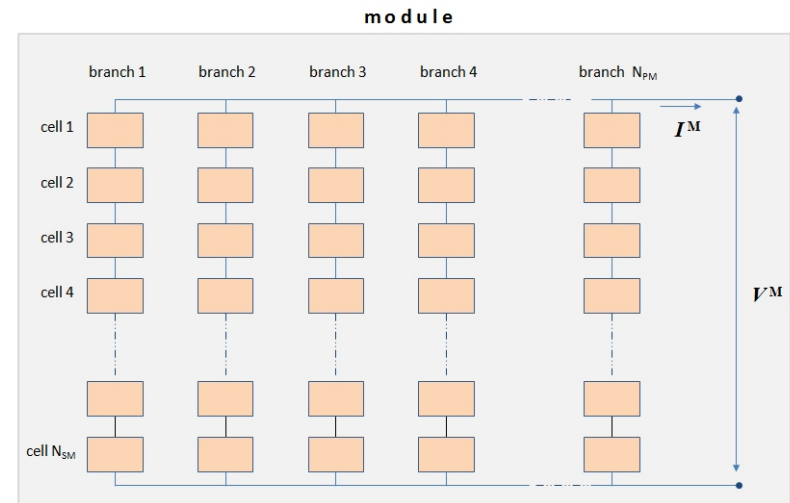
Figure 12: Solar cell array consists of Mp(N_{PM}) parallel branches, with Ms(N_{SM}) modules in series in each branch.

2.3 DC-DC Boost Converter

A boost converter is shown in Figure 13 is a type of DC-to-DC converter that is used to increase a lower voltage level to a higher voltage level. In the context of a standalone solar system, a boost converter is utilized to raise the lower voltage output from the PV panels to a level suitable for charging the battery or powering the load. This converter operates by storing energy in an inductor during the ON state and then transferring it to the output during the OFF state. By stepping up the voltage, the boost converter enables efficient energy utilization and maximizes the overall system performance[19]. The equations for the boost converter are:
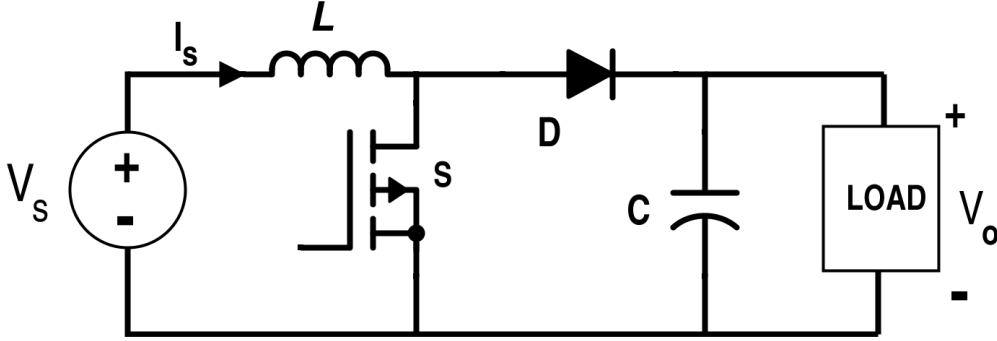
Figure 13: Boost converter.

$$\frac{di}{dt} = \frac{1}{L}(v_{\text{in}} - v_{\text{out}}) \tag{2.11}$$

$$\frac{dv_{\text{out}}}{dt} = \frac{1}{C}\left(\frac{1}{i}\frac{di}{dt} - \frac{v_{\text{out}}}{R}\right) \tag{2.12}$$

$$\frac{v_{\text{out}}}{v_{\text{in}}} = \frac{1}{1-D} \tag{2.13}$$

- i: Inductor current.

- v_{in}: Input voltage.

- v_{out}: Output voltage.

- L: Inductance.

- C: Capacitance.

- R: Load resistance.

- D: Duty cycle.

2.4 Battery Model

The most common type of storage used in a PV system is a lead acid battery. Lead acid batteries' primary use is to supply and store energy in a photovoltaic system. Chemical energy can be transformed to electrical energy and vice versa. The following reactions can be used to explain electrochemical reactions[20]:

$$\text{Overall Reaction:} \quad PbO2 + Pb + 2H2SO4 \rightarrow 2PbSO4 + 2H2O \tag{2.14}$$
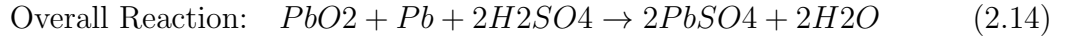
During each time step, the state of charge SOC (t) (per unit) was calculated from the previous time step SOC, adding or subtracting the charge of the battery current[7]:

$$SOC(t) = SOC(t - \Delta t) + \int_{t-\Delta t}^{t} \frac{I_b(\tau)}{C_N} d\tau \tag{2.15}$$

where:

- Δt is the length of the time step in hours.

- $I_b(\tau)$ (as given by Equation (2.13)) is the current that effectively affects the battery charge.

- C_N is the nominal capacity of the battery in Ampere-hours (Ah).

- τ is the time between $t - \Delta t$ and t.

The battery current $I_b(t)$ is calculated as[7]:

$$I_b(t) = \begin{cases} I_{bat}(t) \cdot \eta_{bat\_ch} & \text{if } I_{bat}(t) > 0 \text{ (charge)} \\ \frac{I_{bat}(t)}{\eta_{bat\_d}} & \text{if } I_{bat}(t) < 0 \text{ (discharge)} \end{cases} \quad (2.16)$$

where

- $I_{bat}(t)$ (positive for charging, negative for discharging) is the battery current.

- η_{bat_ch} is the charging efficiency.

- η_{bat_d} is the discharging efficiency.

Usually, both efficiencies are considered to be the same, equal to the square root of the roundtrip efficiency.
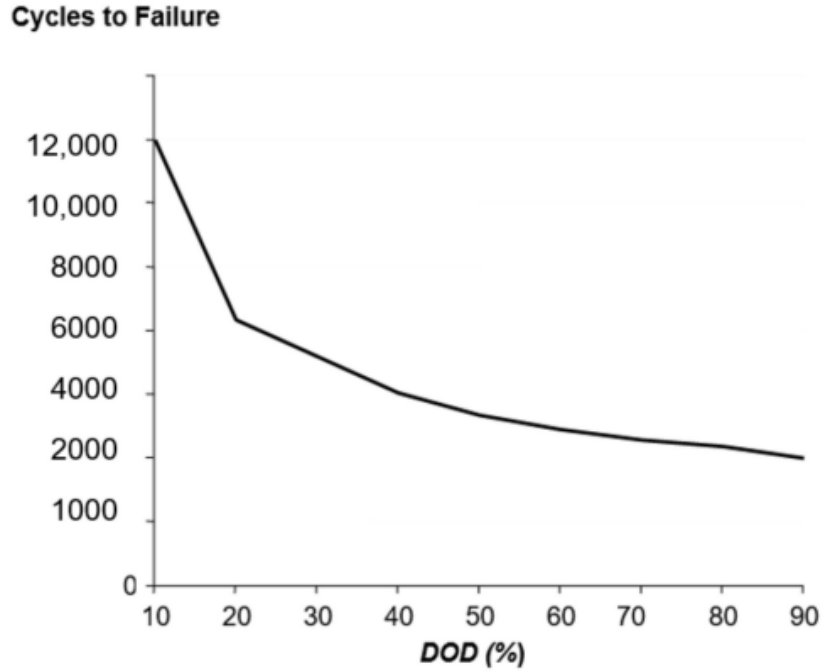
Cycles to Failure

Figure 14: Lead-acid battery: cycles to failure vs. depth of discharge (DOD).

According to the weighted Ah-throughput model put out by Schiffer et al., operating circumstances are often more demanding than those employed in typical cycle and float lifespan studies[7]. To simulate the capacity loss caused by various aging mech-

anisms, this model incorporates weighting variables for charge throughput across battery life. The DOD, the current rate, the acid stratification, and the amount of time since the last full charging all affect these weights[7]. Battery voltage at each time step was calculated depending on if the battery was charging or discharging if $I_{bat}(t) > 0$ (charging), or $I_{bat}(t) < 0$ (discharging), Eq. 2.17, using shepherd model [21]

$$
V_b(t) = \begin{cases} V_0 - g \cdot \text{DOD}(t) + \rho_c(t) \cdot \frac{I_{\text{bat}}(t)}{C_N} + \rho_c(t) \cdot M_c \cdot \frac{I_{\text{bat}}(t)}{C_N} \cdot \frac{\text{SOC}(t)}{C_c - \text{SOC}(t)}, \cdot \\ \\ V_0 - g \cdot \text{DOD}(t) + \rho_d(t) \cdot \frac{I_{\text{bat}}(t)}{C_N} + \rho_d(t) \cdot M_d \cdot \frac{I_{\text{bat}}(t)}{C_N} \cdot \frac{\text{DOD}(t)}{C_d(t) - \text{DOD}(t)}. \end{cases}
$$
(2.17)

In these equations:

- $Vb(t)$ represents the battery voltage at time t.,

- $V0$ is the open-circuit equilibrium cell voltage at the fully charged state.,

- g is an electrolyte proportionality constant,

- $DOD(t)$ is the depth of discharge at time t,

- $\rho_c(t)$ and $\rho_d(t)$ represent the aggregated internal resistance during charge or discharge,

- Mc and Md are coefficients related to internal resistance.

- CN is the nominal capacity of the battery,

- $SOC(t)$ is the state of charge at time t,

- Cc and $Cd(t)$ represent the normalized capacity of the battery during charge or discharge.

The depth of discharge (DOD) can be expressed in terms of the state of charge

(SOC) using the equation:

$$DOD = 100\% - SOC \tag{2.18}$$

The transformation of active chemicals is proportional to the DOD during charging and discharging once the other operation circumstances are known. Figure 14 illustrates how a lead-acid battery's cycle life varies with DOD. It was observed that the battery cycle life obviously decreases with increasing DOD[22].

2.5   DC-DC Buck-Boost Converter

Bidirectional DC/DC converters act as a connection between a storage device and the DC link, facilitating the charging and discharging of these storage devices. The BDCs can function in two modes depending on the battery voltage. When the DC link voltage is higher than the battery voltage, the converter operates in Boost mode, supplying power to the DC link. Conversely, when the battery voltage is lower than the DC link voltage, the converter operates in Buck mode, allowing the battery to be charged using any excess power from the DC link.
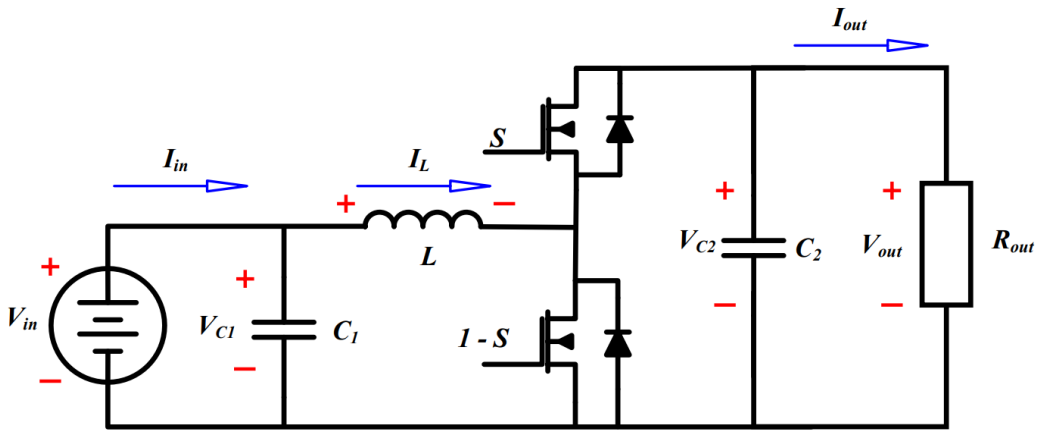
Figure 15: Bidirectional Buck-Boost converter.

The BDC converter topology consists of an inductor, two capacitors, and two switching transistors. The diode of the switching transistor is crucial in the circuit design

as it enables bidirectional current flow between the DC link and the battery storage device. The circuit schematic of the bidirectional Buck-Boost converter is depicted in Figure 15 [23].

By analyzing the ON and OFF switching states of the bidirectional Buck-Boost converter, we can derive the dynamic state space equations. These equations describe the behavior of the converter during operation. The dynamic equations of the bidirectional Buck-Boost converter can be represented by equations[23] :

$$\frac{dI_L}{dt} = \frac{V_{C1}}{L} - \frac{V_{C2}}{L} \cdot (1 - S) \tag{2.19}$$

$$\frac{dV_{C1}}{dt} = \frac{I_{in}}{C_1} - \frac{I_L}{C_1} \tag{2.20}$$

$$\frac{dV_{C2}}{dt} = \frac{I_L}{C_2} \cdot (1 - S) - \frac{V_{C2}}{C_2 \cdot R_{out}} \tag{2.21}$$

where:

- I_L is the inductor current.

- V_{C1} and V_{C2} are the voltages across capacitors C_1 and C_2, respectively.

- S is the switch state.

- I_{in} is the input current.

- L is the inductance.

- C_1 and C_2 are the capacitances.

- R_out is the load resistance.

The duty cycle of BDCs can be represented as follow:

$$\frac{V_{out}}{V_{in}} = \frac{D}{1-D} \tag{2.22}$$

The duty cycle (D) in a DC-DC converter represents the fraction of time during which the switch is ON. It can be calculated using the following equation:

$$D = \frac{T_{on}}{T_{on} + T_{off}} \tag{2.23}$$

where T_{ON} is the ON time of the switch (the time the switch is closed) and T_{OFF} is the OFF time of the switch (the time the switch is open). The duty cycle is typically expressed as a decimal fraction between 0 and 1, where $0 \leq D < 1$. The specific value of the duty cycle will depend on the desired output voltage, input voltage, and the operating conditions of the converter. It can be adjusted to control the output voltage or power conversion ratio of the DC-DC converter.

2.6 PMSG Model

he provided equations describing the modeling of a Permanent Magnet Synchronous Generator (PMSG) in the d-q rotating frame(Figure 16). The equations are as follows[24]:

- Stator voltages:

$$\begin{cases} V_{sd} = Rs \cdot isd + \frac{d\Psi_d}{dt} - \omega_r \cdot \Psi_q \\ V_{sq} = Rs \cdot isq + \frac{d\Psi_q}{dt} + \omega_r \cdot \Psi_d \end{cases} \tag{2.24}$$

- Stator flux components:

$$\begin{cases} \Psi_d = L_d \cdot isd + \Phi_f \\ \Psi_q = L_q \cdot isq \end{cases} \tag{2.25}$$

The above equations allow writing:

$$\begin{cases} V_{sd} = Rs \cdot isd + L_d \cdot \frac{di_{sd}}{dt} - \omega_r \cdot L_q \cdot isq \\ V_{sq} = Rs \cdot isq + L_q \cdot \frac{di_{sq}}{dt} + \omega_r \cdot L_d \cdot isd + \omega_r \cdot \Phi_f \end{cases} \tag{2.26}$$

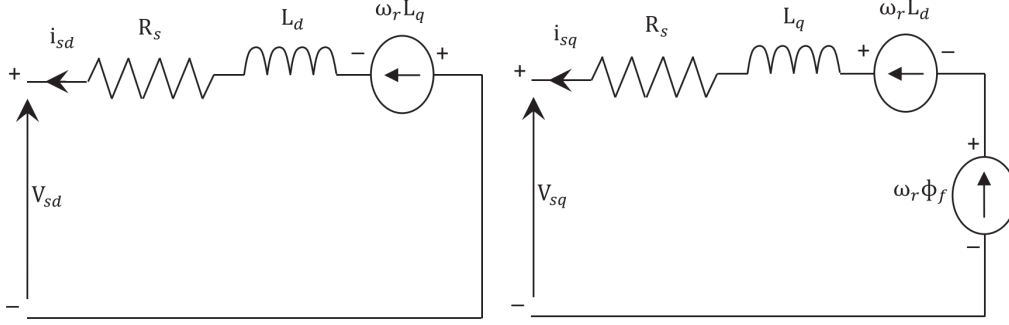The PMSG model in the rotating frame d-q is represented by Figure . The mechan-

Figure 16: d-q model of PMSG in synchronous reference frame.

ical and electromagnetic equations that describe the energy conversion system are determined by the following relationships.

$$\begin{cases} T_{tur} - T_{em} = J \cdot \frac{d\Omega}{dt} + f_c \cdot \Omega \\ T_{em} = \frac{3}{2} p (L_d - L_q) \cdot isd \cdot isq + isq \cdot \Phi_f \end{cases} \tag{2.27}$$

The active and reactive powers equations of the generator can be expressed as follows:

$$\begin{cases} P_{gen} = \frac{3}{2} (V_{sd} \cdot isd + V_{sq} \cdot isq) \\ Q_{gen} = \frac{3}{2} (V_{sq} \cdot isd + V_{sd} \cdot isq) \end{cases} \tag{2.28}$$

- Rs: Stator resistance

- d, q: Stator flux components

- Ld, Lq: d and q-axis inductances

- r: Rotor angular velocity

- f: Permanent magnet flux

- Ttur: Turbine torque

- Tem: Electromagnetic torque

- J: Moment of inertia

- fc: Coefficient of friction

- : Mechanical angular velocity

- p: Number of pole pairs

2.7   DC-AC Inverter

In many industrial and commercial applications, three-phase AC power is preferred due to its higher efficiency and ability to power motors, pumps, and other equipment more effectively. A DC-AC 3-phase converter(Figure 17)facilitates the utilization of DC power in these applications by converting it into three-phase AC power.
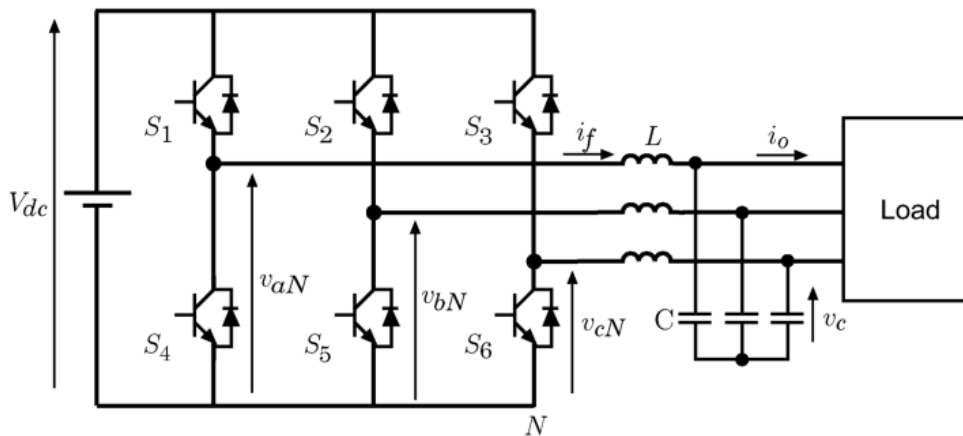
Figure 17: DC-AC Inverter.

Regarding the number of IGBTs, a standard 3-phase bridge inverter configuration utilizes six IGBTs, with each phase leg consisting of an upper and lower IGBT connected in a bridge configuration. This arrangement allows for the control of current flow in each phase and enables the generation of the three-phase AC output.

The power circuit of a three-phase voltage-source inverter, which is shown in Figure
. In this particular scenario, the load is assumed to be unidentified, while the models
for the converter and filter are provided.

Additionally, the two switches in each leg of the converter operate in a complementary manner to prevent short-circuit situations. As a result, the switching states of
the converter can be represented by three binary switching signals, namely Sa, Sb,
and Sc as follows [25].:

$$Sa = \begin{cases} 1, & \text{if S1 is ON and S4 is OFF} \\ 0, & \text{if S1 is OFF and S4 is ON} \end{cases}$$

$$Sb = \begin{cases} 1, & \text{if S2 is ON and S5 is OFF} \\ 0, & \text{if S2 is OFF and S5 is ON} \end{cases}$$

$$Sc = \begin{cases} 1, & \text{if S3 is ON and S6 is OFF} \\ 0, & \text{if S3 is OFF and S6 is ON} \end{cases}$$

These switching states can be expressed in vectorial form, specifically in the $\alpha\beta$
reference frame, using the following transformation:

$$\mathbf{S} = \frac{2}{3}(S_a + aS_b + a^2 S_c) \equiv S_\alpha + jS_\beta, \tag{2.29}$$

$$\begin{bmatrix} S_\alpha \\ S_\beta \end{bmatrix} = \begin{bmatrix} \frac{2}{3} & -\frac{1}{2} & -\frac{1}{2} \\ 0 & \frac{\sqrt{3}}{2} & -\frac{\sqrt{3}}{2} \end{bmatrix} \begin{bmatrix} Sa \\ Sb \\ Sc \end{bmatrix} =: \mathbf{T_c}(\text{Clarke transformation}), \tag{2.30}$$

where $a = e^{j(2\pi/3)}$. It is assumed that the switching devices are ideal switches, and
thus, the process of switching ON/OFF is not taken into consideration. The possible

output voltage space vectors generated by the inverter can be obtained as follows:

$$\mathbf{v}_i = \frac{2}{3}(v_{aN} + av_{bN} + a^2 v_{cN}), \tag{2.31}$$

- v_{aN}, v_{bN}, and v_{cN} represent the phase-to-neutral voltages of the inverter.

On the other hand, we can define the voltage vector $\mathbf{v}_i$ in terms of the switching state vector $\mathbf{S}$ and the DC-link voltage V_{dc} as:

$$\mathbf{v}_i = V_{dc}\mathbf{S}. \tag{2.32}$$

The Figure 18 illustrates the eight switching states and, consequently, the eight voltage vectors generated by the inverter using equations 2.29 and 2.31. These voltage vectors are obtained by considering all possible combinations of the switching signals S_a, S_b, and S_c. It is important to note that out of the eight voltage vectors, only seven different voltage vectors are considered as possible outputs since $v_0 = v_7$.
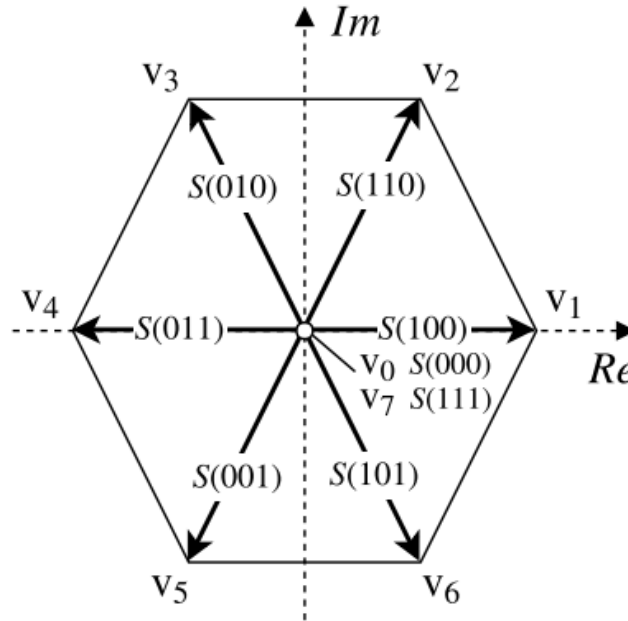
Figure 18: Possible combinations of the switching signals, and their corresponding voltage vectors generated.

Similarly, as expressed in equation 2.29, the filter current i_f, the output voltage v_c, and the output current i_o can be represented in vectorial form as:

$$i_f = \frac{2}{3}(i_{fa} + ai_{fb} + a^2 i_{fc}) \equiv i_{f\alpha} + ji_{f\beta}, \tag{2.33}$$

$$v_c = \frac{2}{3}(v_{ca} + av_{cb} + a^2 v_{cc}) \equiv v_{c\alpha} + jv_{c\beta}, \tag{2.34}$$

$$i_o = \frac{2}{3}(i_{oa} + ai_{ob} + a^2 i_{oc}) \equiv i_{o\alpha} + ji_{o\beta} \tag{2.35}$$

2.8 Conclusion

In Chapter Two, we focused on modeling the components of our hybrid energy system and the converters used for energy conversion. We utilized a DC-DC boost converter for the PV system to optimize power generation, a DC-DC buck-boost converter for the battery system to ensure efficient energy storage, and a DC-AC inverter to transfer DC power to the AC bus for load supply. These modeling efforts enable efficient energy conversion, utilization of renewable sources, and reliable load supply.

Chapter3

Control and Energy Management

of HRES

Chapter 3

Control and Energy Management of HRES

3.1 Introduction

In the previous chapter, we extensively modeled and discussed the different components of our Hybrid Renewable Energy System (HRES). Now, we delve into a crucial aspect of the HRES: the control of each component. Effective control strategies are essential for ensuring optimal performance, efficiency, and reliability of the system.

In this chapter, we focus on exploring the control methodologies employed for managing and regulating the operation of various HRES components. Each component, including the PV (photovoltaic) system, battery storage, diesel generator, and any other auxiliary units, requires a tailored control approach to achieve seamless integration and coordinated operation.

3.2 MPPT Method

The control of the PV system involves implementing algorithms that maximize energy harvesting from solar radiation. It includes MPPT (Maximum Power Point

Tracking) techniques to optimize the power output of the PV panels, considering factors such as varying weather conditions and shading effects.

The most commonly employed algorithm for Maximum PowerPoint (MPP) tracking is the Perturb and Observe (P&O) algorithm. The fundamental principle of this algorithm involves perturbing the system by adjusting the duty cycle of the converter and observing the resulting effect on the output power.

When using the P&O algorithm, if the current power reading (P(k)) is higher than the previous power reading (P(k-1)), the perturbation is continued in the same direction. Conversely, if the current power reading is lower, the perturbation direction is inverted[26].

Figure 19 presents a flowchart that illustrates the P&O technique.
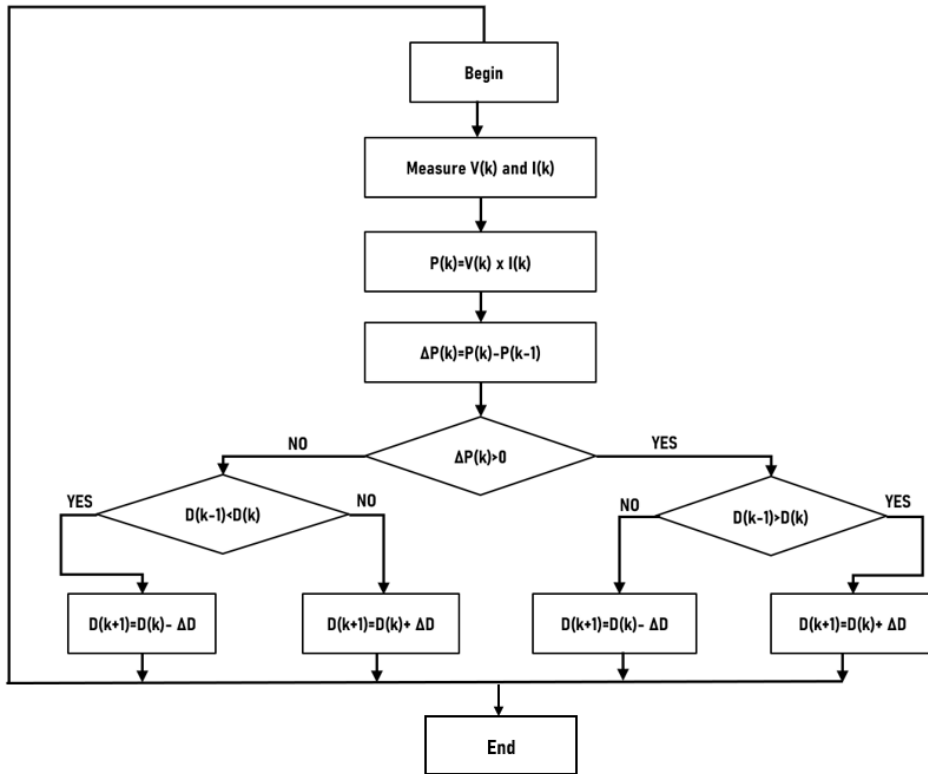
Figure 19: Flowchart of the Perturb and Observe method.

3.3 Buck-Boost Converter Control

The bidirectional converter's control strategy relies on managing the charging and discharging of the battery at a specified Dclink voltage. Figure 20 illustrates the control structure of the bidirectional DC-DC converter.
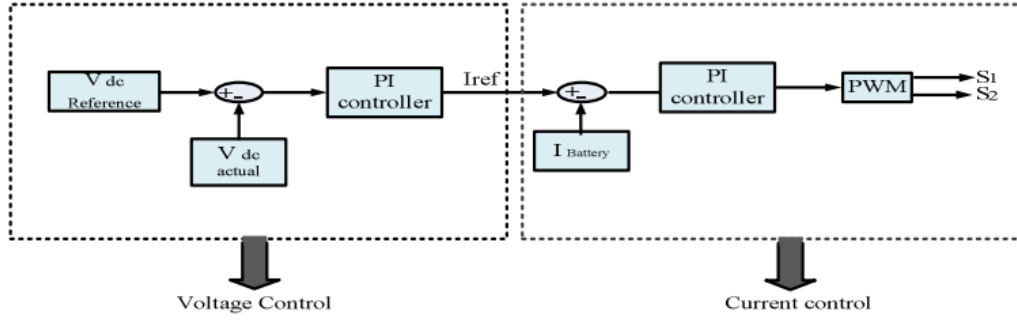
Figure 20: Control algorithm for dc-dc buck-boost converter.

•Step-down mode (Charging): At higher irradiance the generated voltage will be more than the reference value DC-link voltage and the excess voltage will be more than the load demand. Hence, the battery system will get charged through DC-link.

• Step-up mode (Discharging): At lower irradiance the voltage generated will be less than the reference value of the DC-link voltage in this case the battery will charge the DC-link to maintain the DC-link the voltage at reference value.

The voltage control scheme employed for DC-Link is to stabilize the DC- link Voltage during Load change and PV irradiance change the DC-link PI controller maintains the reference voltage.[27].

3.4 Fuzzy Logic Energy Management

Fuzzy logic energy management in standalone systems optimizes energy utilization through intelligent control decisions based on inputs such as power generation, consumption, battery state of charge, and relevant parameters. It aims to maximize efficiency, minimize non-renewable energy usage, and balance power distribution among components for improved system performance.

The energy management strategy based on fuzzy control is designed as shown in Figure 21 [28].
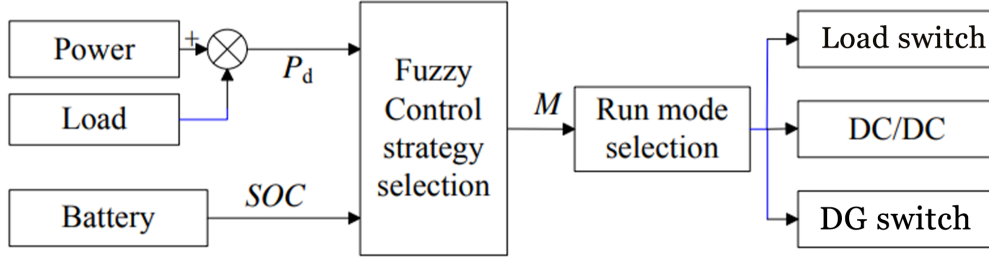
Figure 21: Fuzzy-Controlled energy management diagram.

The defined control process for the fuzzy strategy involves using two inputs for the fuzzy controller: the power difference between the PV power module and the load module, and the battery State of Charge (SOC) from the battery module.

The control signals M for the operation mode selection module is obtained by applying the fuzzy strategy operation.

The fuzzy modeling approach utilizes input and output membership functions to represent the degree of membership of variables in linguistic terms. These membership functions play a key role in fuzzifying the inputs and defining the fuzzy output behavior.

SOC (State of Charge) and Pd (Power demand) are the input variables used in our energy management system. Membership functions are employed to represent the fuzzy sets associated with variables. The input and output membership functions are depicted in Figure 22.
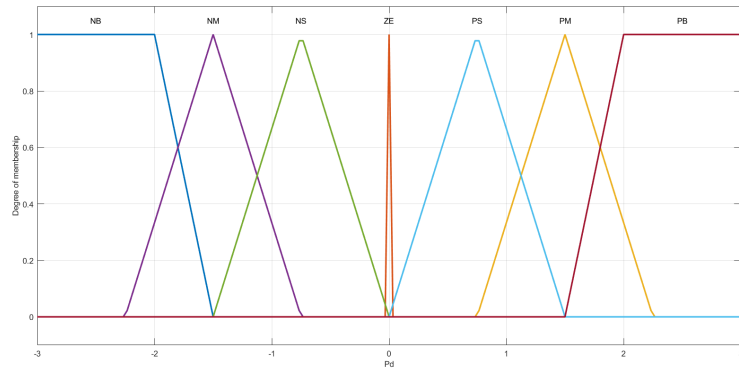
(a) Pd input membership function.
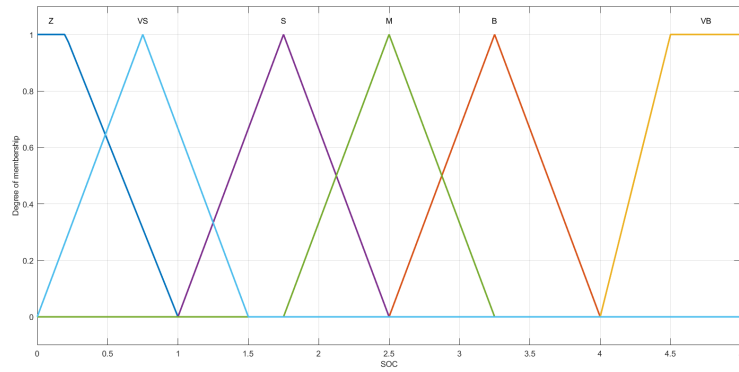
(b) SOC input membership function.
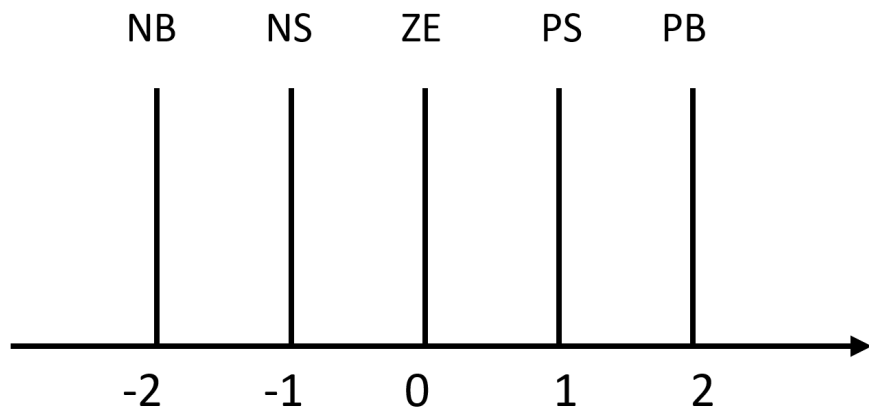
(c) Output membership function.

Figure 22: Output and input membership functions

The fuzzy control rules are designed according to the principles shown in Tab 3.1[28].

M		Pd						
		NB	NM	NS	ZE	PS	PM	PB
SOC	Z	NM	NM	NM	ZE	PS	PS	PS
	VS	NM	NM	NM	ZE	PS	PS	PS
	S	NM	NM	NM	ZE	PS	PS	PS
	M	NM	NM	NM	ZE	PS	PS	PS
	B	NM	NM	NS	ZE	PS	PM	PM
	VB	NS	NS	NS	ZE	PM	PM	PM

Table 3.1: Fuzzy control rules.

NB(Negative Big), NS (Negative Small), NM(Negative Medium),ZE(Zero), PM(Positive Medium),PS(Positive Small) ,PB(Positive Big), Z(Zero), VS(Very Small), S(Small), M(Medium), B(Big), VB(Very Big).

A fuzzy surface graph represents the membership degrees or fuzzy values associated with different points in a two-dimensional space. It visualizes the irregularities or varying heights of the surface, indicating the degrees of membership or fuzziness, as shown in Figure 23
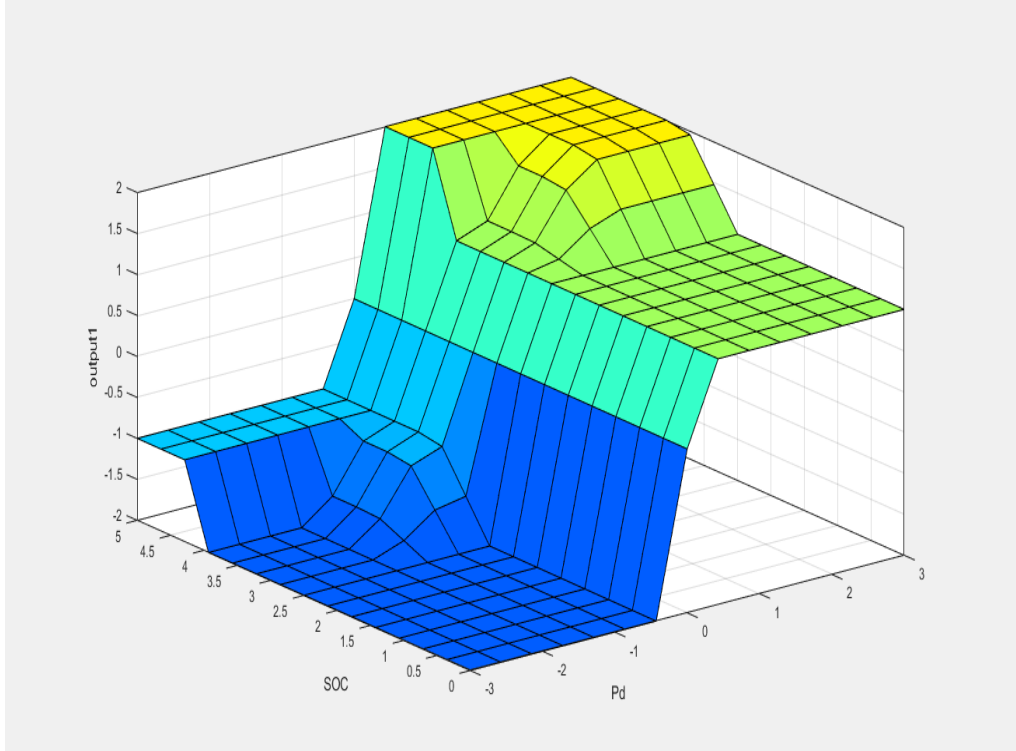
Figure 23: Fuzzy logic surface.

In this module, the control signal M is decomposed into the operation mode selection signal of the diesel generator, the charge/discharge control signal of the battery DC/DC module and the extra load. the output has 5 modes of operation :

- M = −2, $Pd < 0$, $SOC < 0.7$:

    - The DG supplies the load.

    - The secondary load shed

    - The battery starts charging.

- M = −1, $Pd < 0$, $SOC > 0.7$:

    - The PV and the battery supply power to the load.

- M = 0, $Pd = 0$:

    - The PV only supplies the load.

- M = 1, $Pd > 0$, $SOC < 0.9$:

    - The PV supplies the load.

    - The PV charges the battery.

- M = 2, $Pd > 0$, $SOC > 0.9$:

    - The PV supplies the load.

3.5   Standalone Inverter Control

To control the inverter, voltage-oriented control (VOC) is commonly employed. VOC is a control strategy that focuses on regulating the voltage and current of the inverter's output.

The decoupled controller's block diagram is illustrated in the accompanying Figure 24.
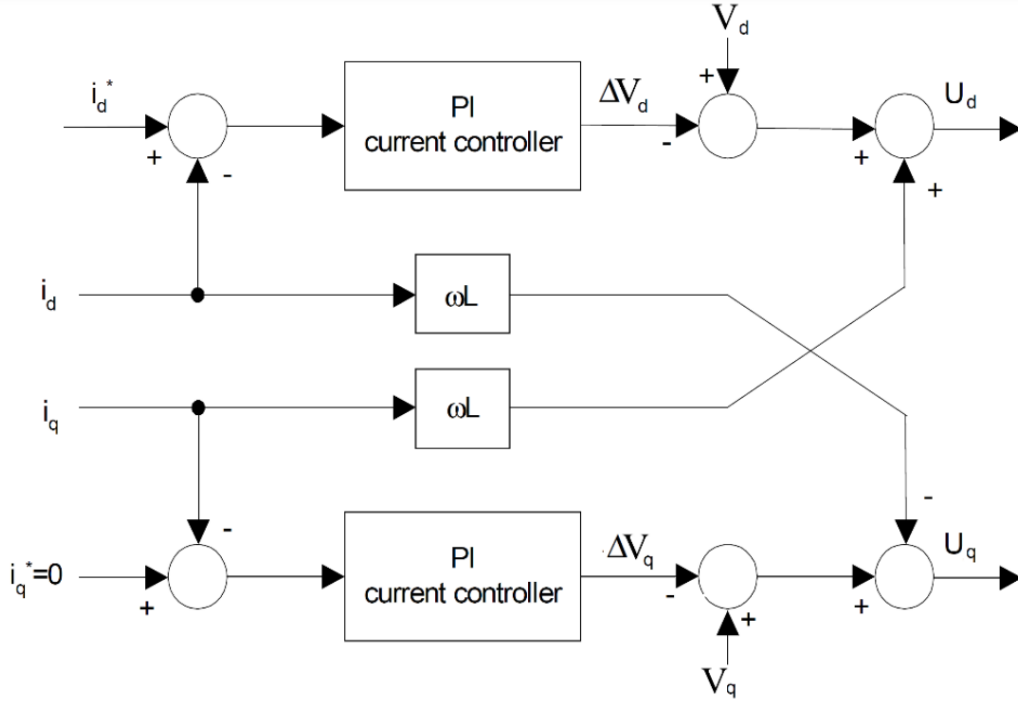
Figure 24: VOC block scheme

The VOC strategy is known for its reliable performance and satisfactory static and dynamic response at a fixed switching frequency and low sampling frequency[29]. this technique used decoupled pi controllers to control the current components (Id, Iq) and generate a reference voltages (Vd, Vq) to be fed to the PWM block after coordinate transformation (dqo-abc) to produce the inverter switching states

3.5.1   Sinusoidal PWM

Sinusoidal modulation is based on a triangular carrier signal. The concept involves comparing three sinusoidal reference voltages (Ua*, Ub*, and Uc*) to this triangular wave. By making these comparisons, logical signals Sa, Sb, and Sc are generated, which determine the switching instants of power transistors.

During operation, the constant carrier signal helps concentrate voltage harmonics around the switching frequency and its multiples. This characteristic is beneficial for achieving efficient modulation and reducing unwanted frequency components in the system[30].
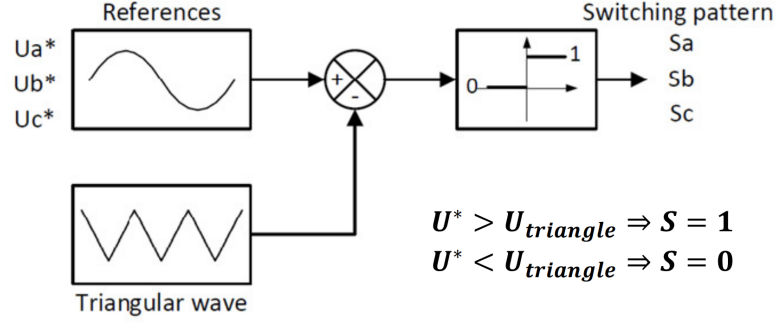
Figure 25: Sinusoidal PWM.
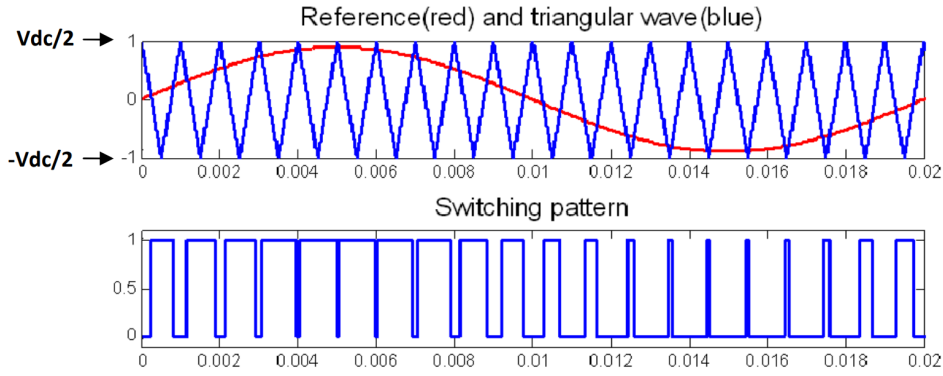
Figure 26: Sinusoidal PWM basic waveforms.

3.6 Conclusion

In this chapter, we extensively discussed the control methodologies employed for managing and regulating various components within the Hybrid Renewable Energy System (HRES). We emphasized the importance of tailored control approaches for each component and highlighted the role of fuzzy logic in achieving effective control. Fuzzy logic enabled us to handle uncertainty and imprecise information by incorporating linguistic variables and fuzzy rules into the control decisions. Additionally, we explored voltage and pulse width modulation (PWM) techniques that worked in conjunction with fuzzy logic to regulate power flow and energy conversion processes. These techniques ensured optimal performance and efficiency of the HRES.

Chapter4

Simulation, Results and Discussion

Chapter 4

Simulation, Results and Discussion

4.1   Introduction

In this chapter, the simulation results and their discussion are presented, focusing on the application of the Energy Management System to three distinct scenarios. These scenarios involve variations in irradiances, load demand, and the state of charge of the battery. The main objective is to verify the accuracy and effectiveness of the energy management strategy implemented in the system, which is based on fuzzy logic control. The tests were conducted using the MATLAB/Simulink simulation environment.

4.2   Methodology

In the previous chapter, the fuzzy logic method was introduced. This method takes inputs such as the power difference between the input and output, as well as the State of Charge (SOC) of the battery. Using these inputs and the rules of the fuzzy inference system, the method generates an output that determines the mode of operation for our system. This selected mode then generates control signals, enabling

the control of various elements within the system by facilitating their switching.

4.3   Application

The system incorporates various components including renewable energy resources in the form of a Photovoltaic system (Solar Array), an Energy Storage System (ESS), a Diesel generator, a Three-phase load, Power Electronics devices (Inverters, converters), and an Energy Management system.

The Photovoltaic model consists of a Solar Array of 3.5KW with 8 series modules and 2 parallel strings, as illustrated in the I-V and P-V characteristics Figure 27. The PV characteristics are shown in the Appendix.

The load profile represents the overall energy consumption during the simulation, with each simulation featuring distinct load profiles.

The ESS model, the battery pack has a voltage of 120V and a rated capacity of 250Ah. The state of charge (SOC) of the battery varies in each simulation.
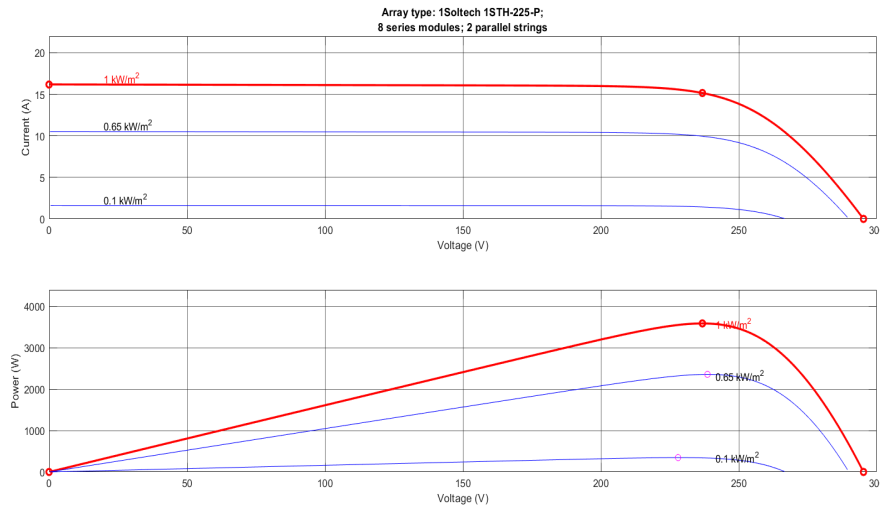
Figure 27: PV array P-V and I-V characteristics.

4.4 Simulation of Different Scenarios.

4.4.1 First Scenario

The PV power is initially set at 3200W(Figure 29) and gradually decreases over time. The state of charge (SOC) is maintained at 90%(Figure 31), while the power demand fluctuates, as depicted in Figure 28 (a). Fuzzy logic and control signals are shown in Figure 30

(a) Power load demand.

(b) PV solar irradiance
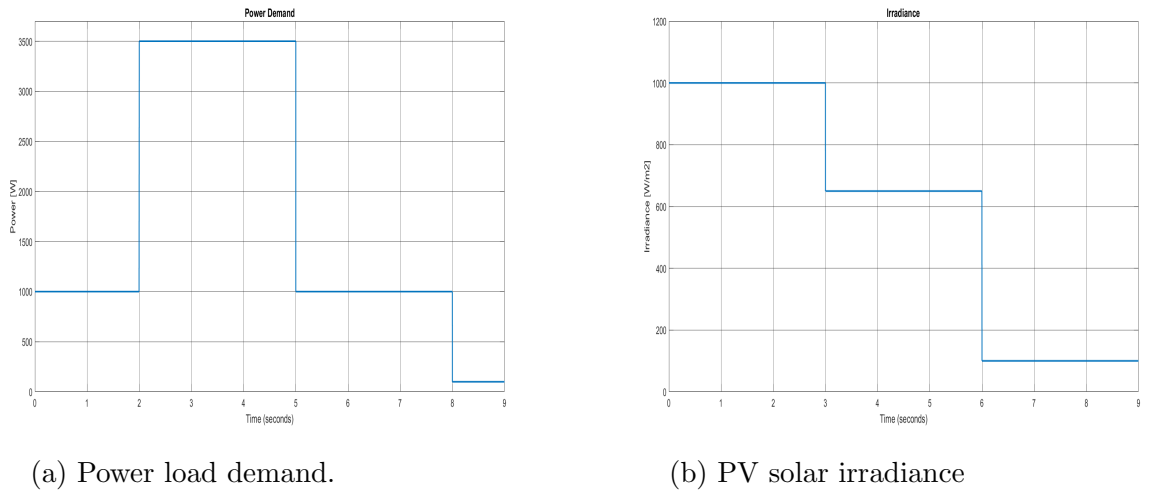
Figure 28: First scenario (a)Load demand,(b)Solar irradiance
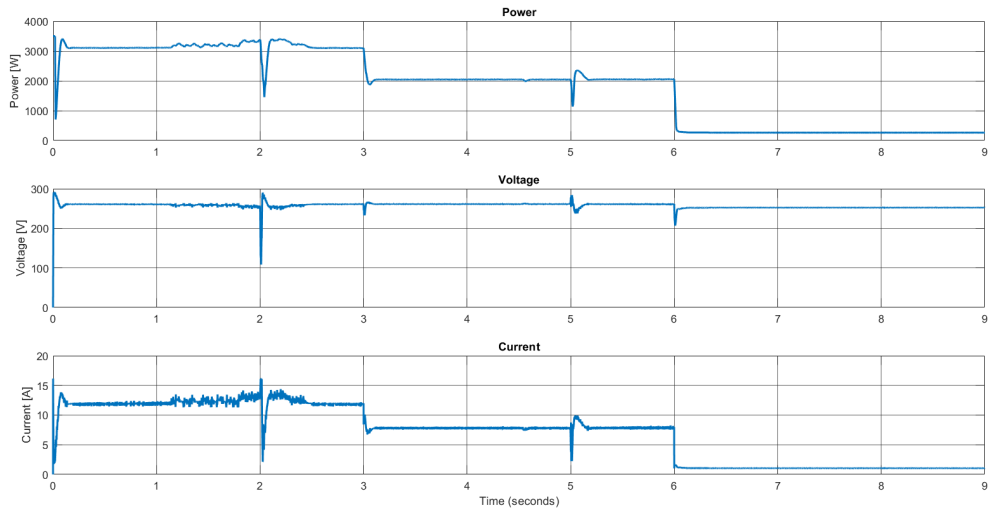
Figure 29: PV power, voltage, and current.

In this scenario, as observed in Figure 30, the system operates in two modes. Mode $M = 2$ is characterized by the PV power supply exceeding the load power demand $(P_d > 0)$ and the state of charge (SOC) being greater than 0.9.

As a result, the PV system directly provides power to the load, while the battery operates without restrictions, either charging or discharging to maintain the DC Link power.

In mode $M = -1$, the power supplied by the PV is less than the load power demand $(P_d < 0)$, but the SOC remains above 0.7. In this case, both the PV system and the battery collaborate to supply power to the load.
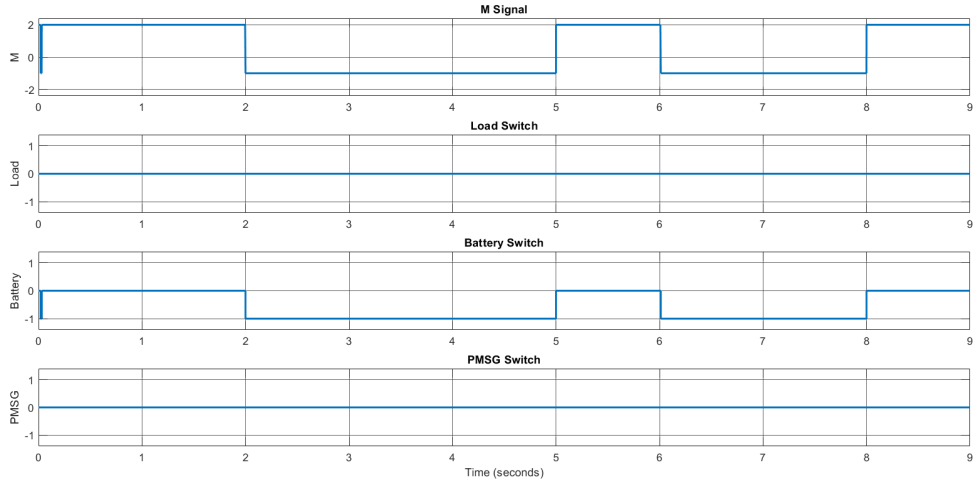
Figure 30: Fuzzy and control signals.

During the specified time intervals, the system operates as follows:

• From 0s to 2s, the PV system supplies power to the load.

• From 3s to 5s, the power demand increases, triggering the fuzzy controller to switch to mode M=-1. Consequently, the battery starts supplying power to meet the load demand.

• From 5s to 6s, the system returns to mode M=2, with the PV system serving as the main power source for the load.

• From 6s to 8s, the PV power output becomes insufficient to meet the demand, prompting the battery to assist in satisfying the load requirement(Figure 31).

• Lastly, when the load demand is very small, the PV system resumes supplying

power to the load.
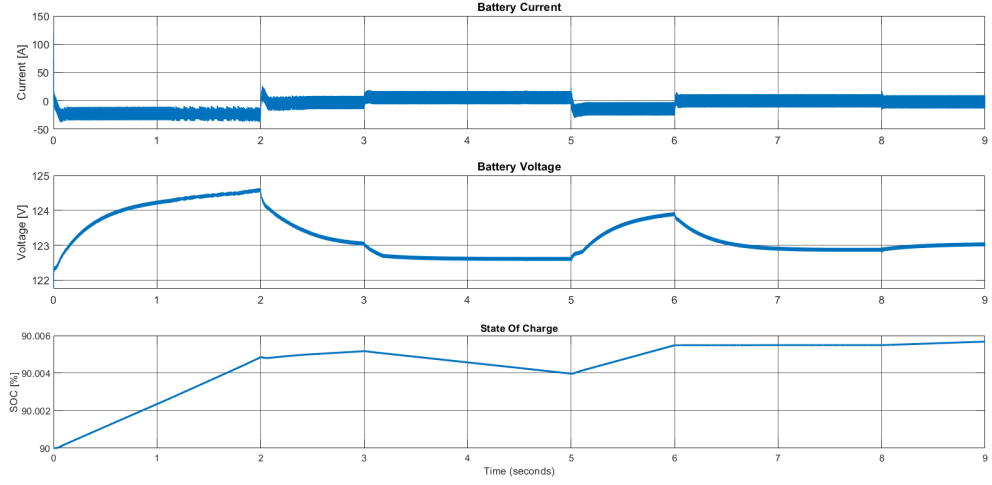
Figure 31: Battery current, voltage and SOC.

The DC Link power (Figure 32)represents the sum of the PV system power and
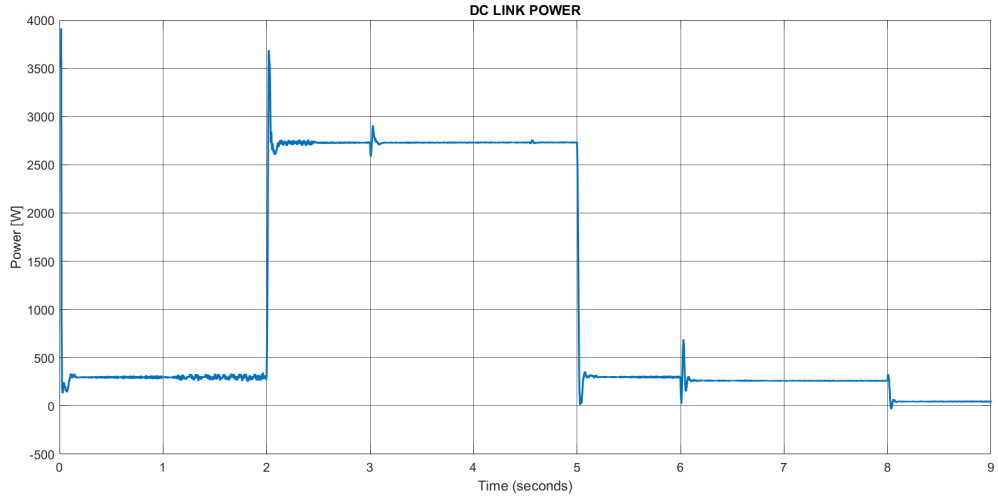
Figure 32: DC link power.

the battery power. Initially, the battery is being charged, resulting in a low DC Link power.

However, as the load demand increases, the power in the DC Link also increases, and the battery charging process is halted(Figure 31). Subsequently, the DC Link power gradually decreases because the PV power decreases and struggles to meet the load demand without requiring the intervention of the battery.
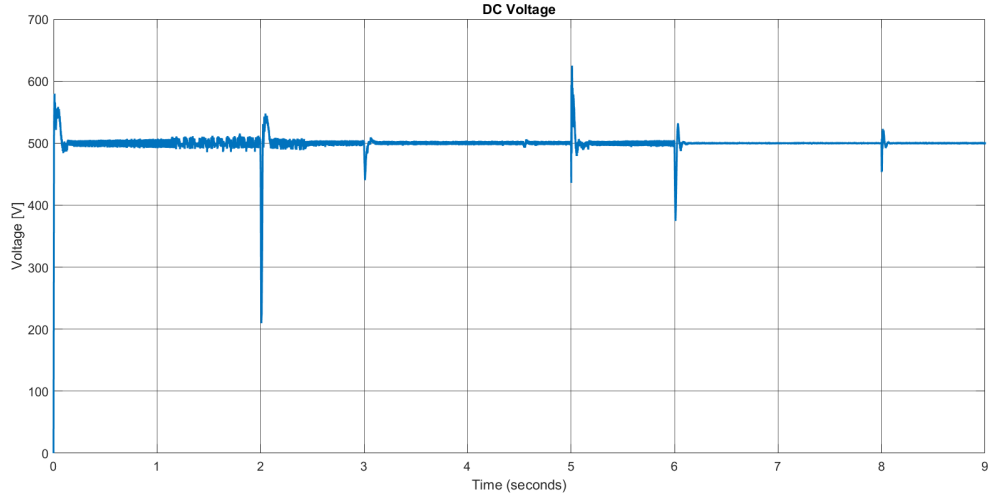
Figure 33: DC link voltage.

The DC Link voltage(Figure 33) is actively maintained at a constant level of 500V with the assistance of the battery control reference voltage. Although it may fluctuate temporarily in response to sudden changes in the system's power, it stabilizes shortly thereafter. This behavior serves as evidence of the effectiveness and accuracy of the implemented control strategy.

The Figures(34, 35, 36) represents the load side results.
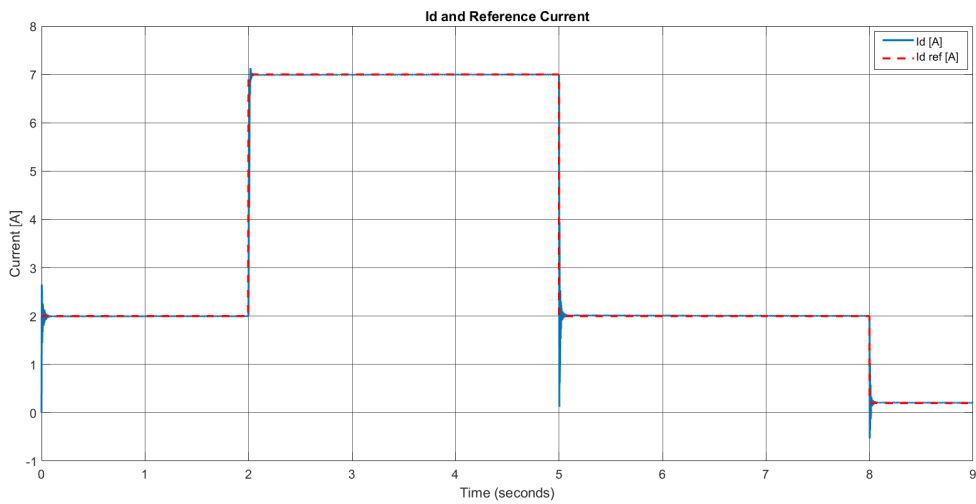
Figure 34: Id and reference current.

The direct current component (Id) utilized in the voltage control strategy for the Three-phase inverter closely approximates the reference current, as illustrated in Figure 34.

As observed in Figure 35, the voltage and current of the output exhibit a responsive behavior to variations in the direct current (Id) that is responsible for voltage control.
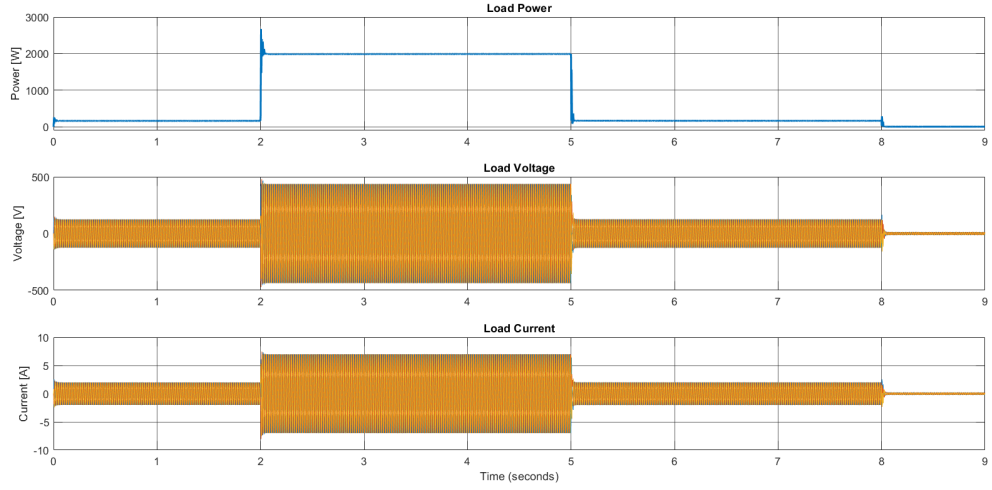
Figure 35: Load power, voltage and current.
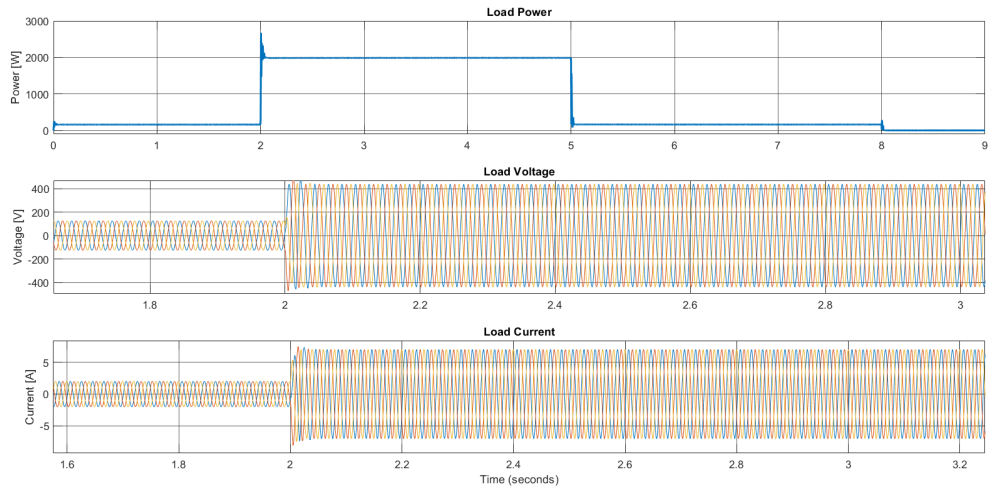
Figure 36: Load power, voltage and current.

4.4.2 Second Scenario

The PV power is set at 3500W(Figure 38), but it gradually decreases over time. The State of Charge (SOC) of the battery is set at 50%(Figure 40). And the power

demand fluctuates, as depicted in Figure 37 (a). Fuzzy logic and control signals are shown in Figure 39.

We used 2 loads:

- three-phase R load 3000W $380V_{\text{rms}}$

- three-phase R load 1000W $380V_{\text{rms}}$
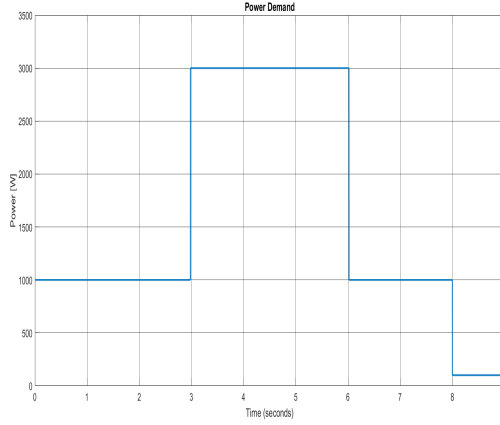
(a) Power load demand.
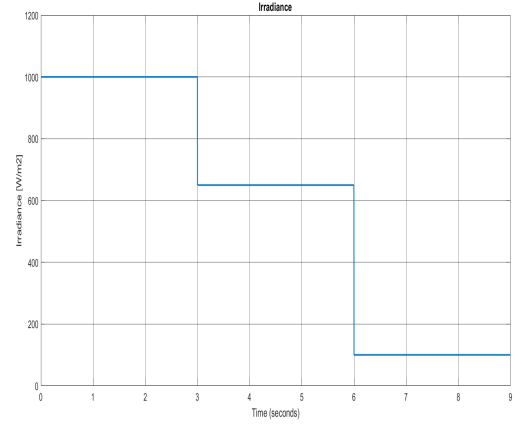
(b) PV solar irradiance.

Figure 37: Second scenario (a)Load demand,(b)Solar irradiance.
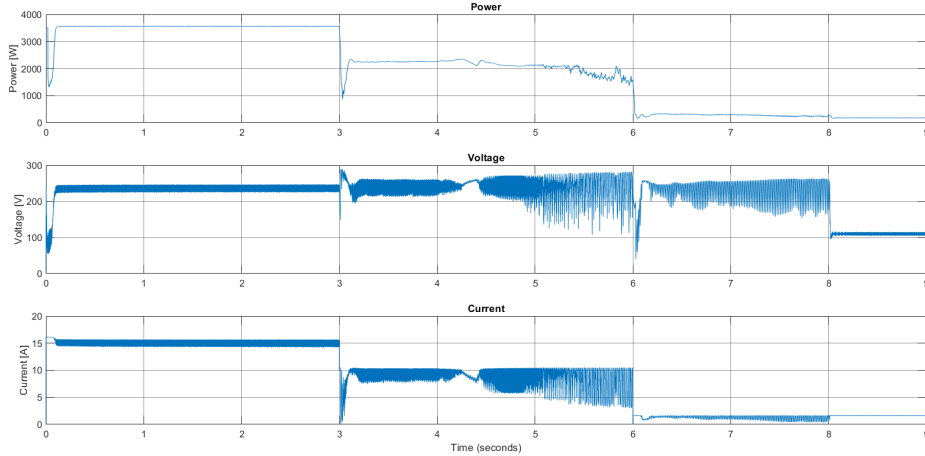
Figure 38: PV power, voltage, and current.

In this scenario, as shown in Figure 39, the modes of operation of the system are $M = 1$ and $M = -2$. In mode $M = 1$, it indicates that the power delivered by the PV exceeds the load power demand ($P_d > 0$), and the State of Charge (SOC) is below 0.9. As a result, power is supplied to the load by the PV, and the battery

is simultaneously being charged(Figure 40). On the other hand, mode $M = -2$ signifies that the power delivered by the load is less than the load power demand ($P_d < 0$), and the SOC is below 0.7. This leads to the shedding of the second load, the intervention of the Diesel engine to compensate for the load demand, and the battery being charged.
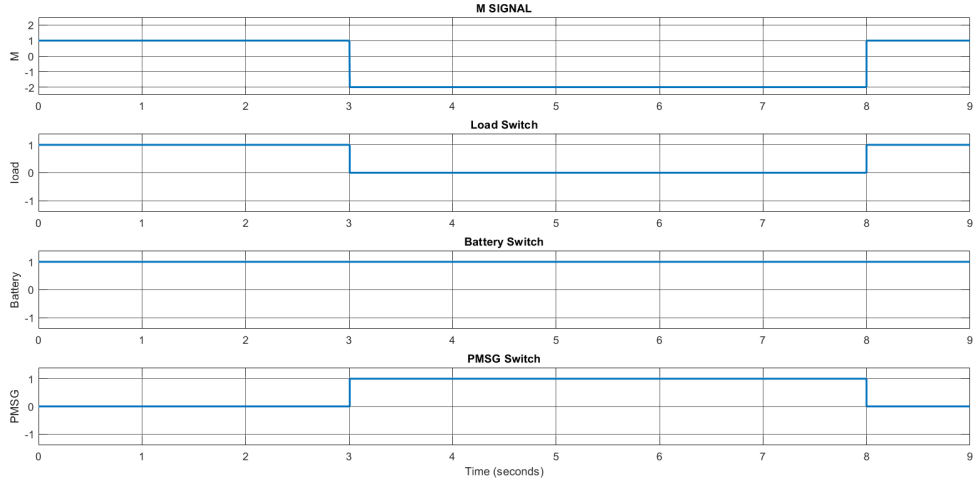

Figure 39: Fuzzy and control signals.

During the specified time intervals, the system operates as follows:

• From 0s to 3s: System operates in mode M=1. PV is the main power source, supplying power to the load and charging the battery.

• From 3s to 8s: Power demand exceeds PV power. Fuzzy controller switches to mode M=-2. Diesel injection occurs, the secondary 1000W load is shed, and the battery charges.

• From 8s to 9s: System operates in mode M=2. PV supplies power to the load, shedded load gets connected again, but the battery starts to discharge due to low DC link power.

In Figure 41, the PV initially charges the battery and powers the load. However, as the demand increases, the PV power decreases while the battery continues to charge. As a result, the DC link power decreases and eventually becomes negative when the PV power drops even further and the load is supplied by the DG, while the
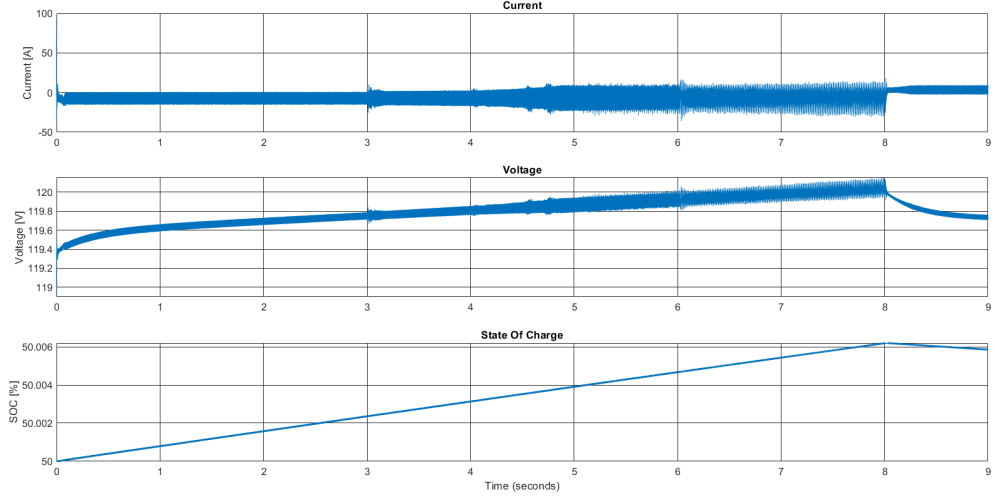
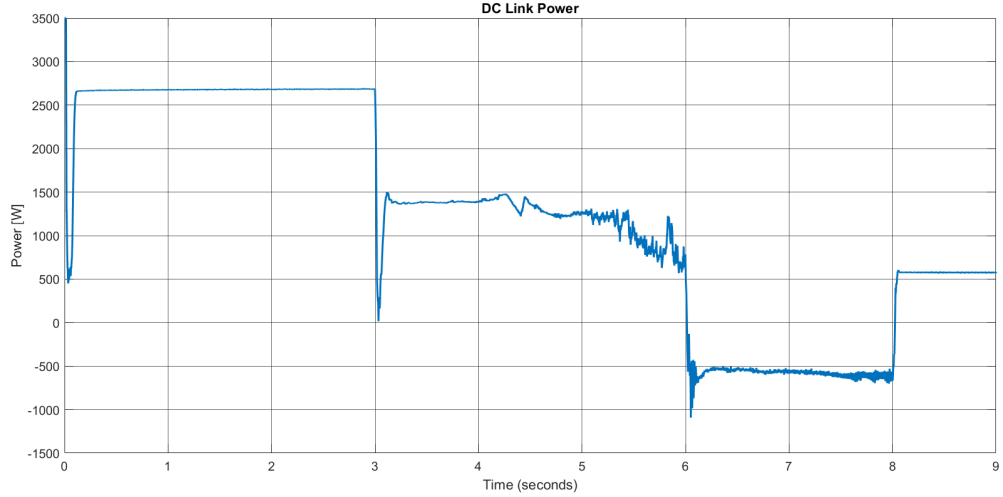Figure 40: Battery current, voltage and SOC.

Figure 41: DC link power.

battery remains charging. Lastly, the DG is disconnected and the battery discharges slightly. Consequently, the DC link power increases, reaching a value of 500W.

The Figures(42, 43) represents the load side results.

In Figure 42, it is noticeable that the Load Power typically aligns with the load demand pattern. However, with the introduction of a second load connection and subsequent shedding, there are slight alterations in the Load Power behavior. Additionally, the voltage and current values align with the reference values set by the Voltage control.
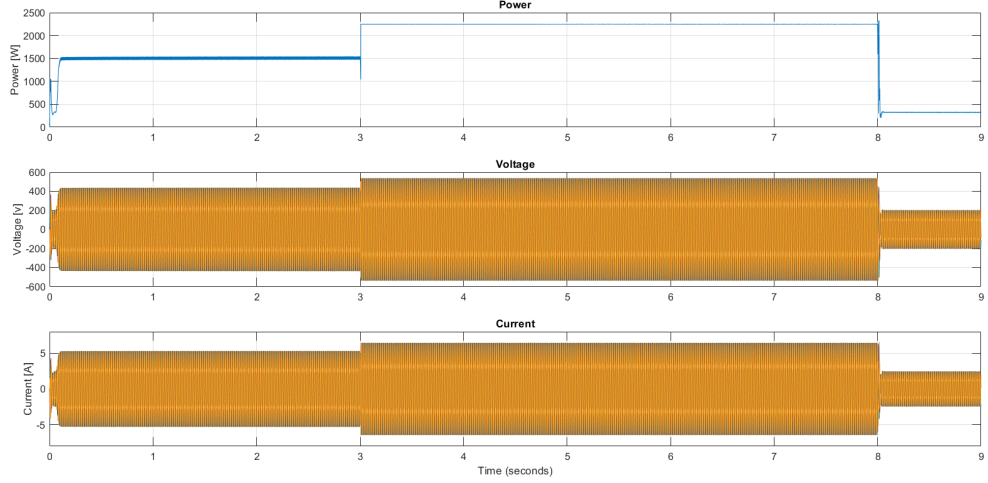
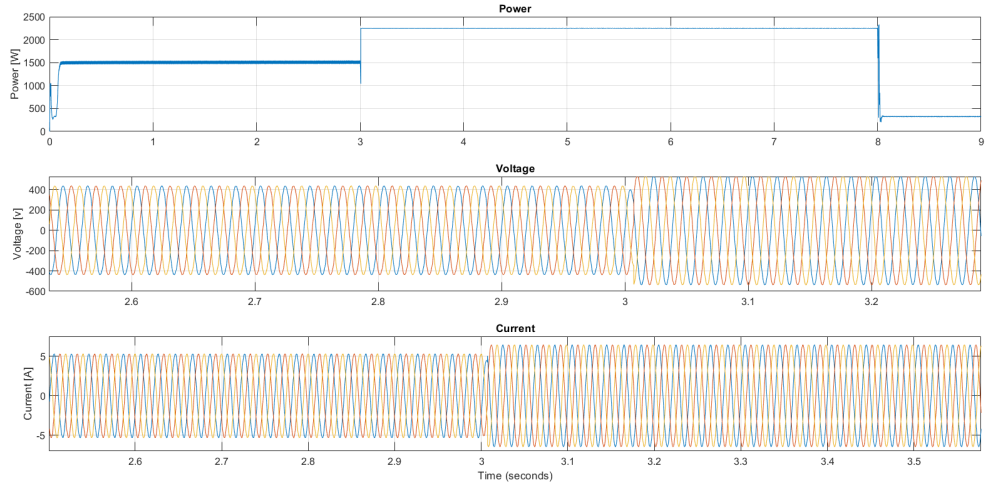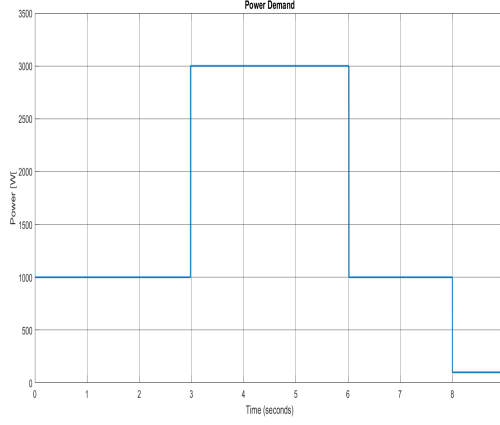Figure 42: Load power, voltage and current.

Figure 43: Load power, voltage and current.

4.4.3 Third Scenario

Different Solar irradiance profile that simulate the insulation variation along a day(Figure 44 (b)).

The PV power starts at 1000W and varies over time(Figure 45). The state of charge is set at 90%(Figure 47), and the power demand fluctuates as shown in Figure 44 (a).Fuzzy logic and control signals are shown in Figure 46.

The modes of operation in this scenario as it can be seen in Figure 46 are M=2 and M=-1, they are explained in the past scenarios.
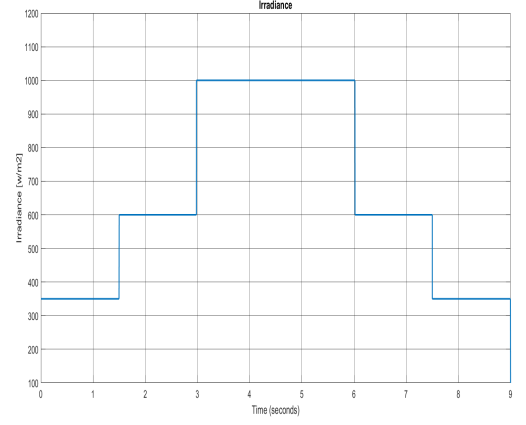
(a) Power load demand.   (b) PV solar irradiance

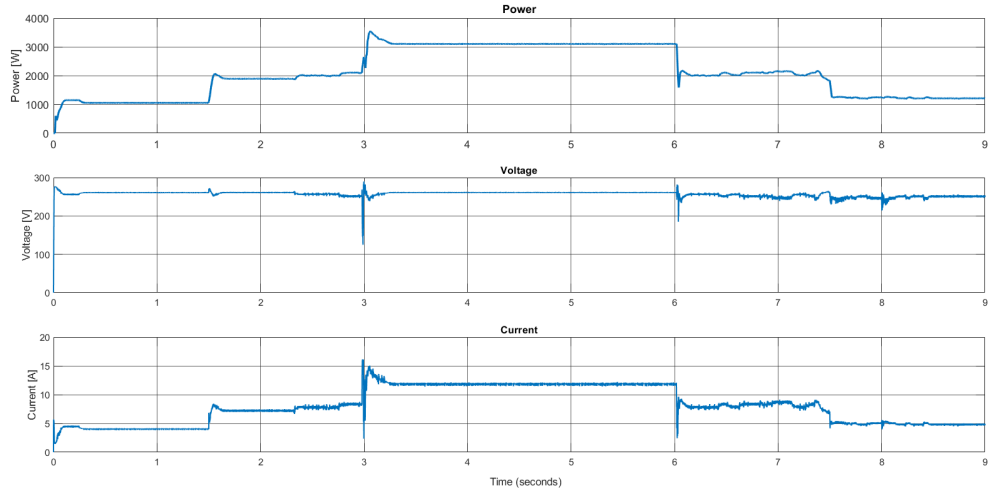Figure 44: Second scenario (a)Load demand,(b)Solar irradiance.

Figure 45: PV power, voltage and current.

From 0s to 3s: System operates in mode M=2. PV is the main power source, supplying power to the load and charging the battery. After reaching 3s the system switches to Mode M=-1 due to the fast change in the load power demand but it shortly recovers back to mode M=2, continuing in this mode until the end of the simulation.
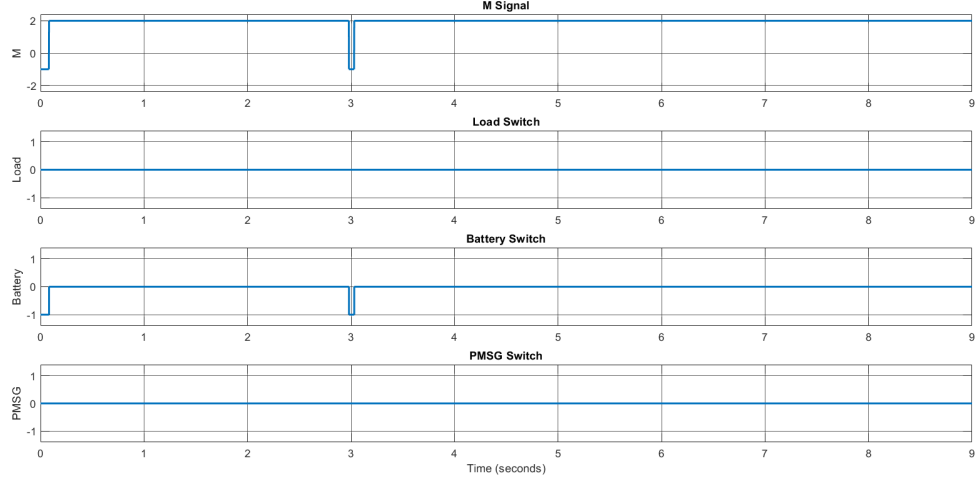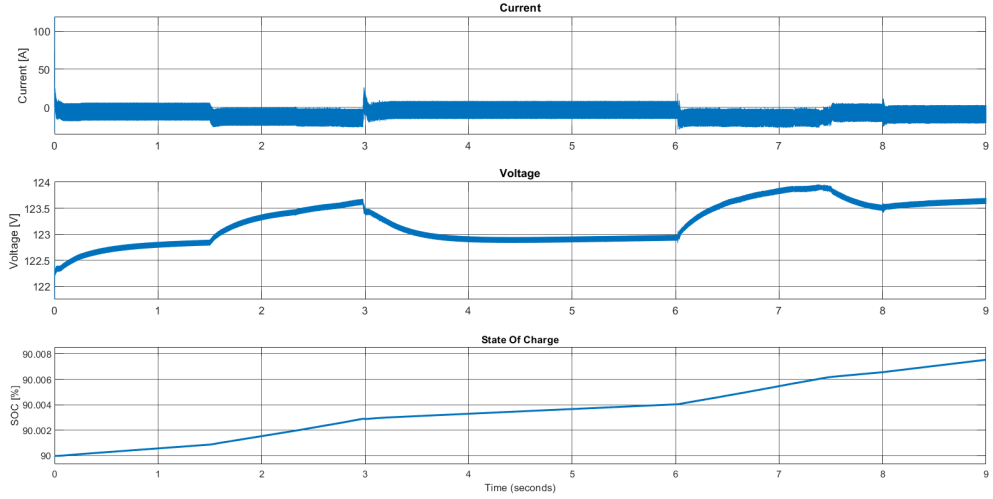
Figure 46: Fuzzy and control signals.

Figure 47: Battery current, voltage and SOC.

Initially, from Figure 48 it can be seen that the DC link power is utilized by both the battery and the load. It responds to variations in the load's power requirements. However, when the PV power increases, the DC link power remains constant and is redirected towards the battery, that can be seen in the SOC slope(Figure 47).

The DC link voltage(Figure 49) is maintained at a steady 500V by the battery control reference voltage. However, it experiences fluctuations whenever there is a sudden change in the system's power but it stabilizes shortly after these fluctuations occur.
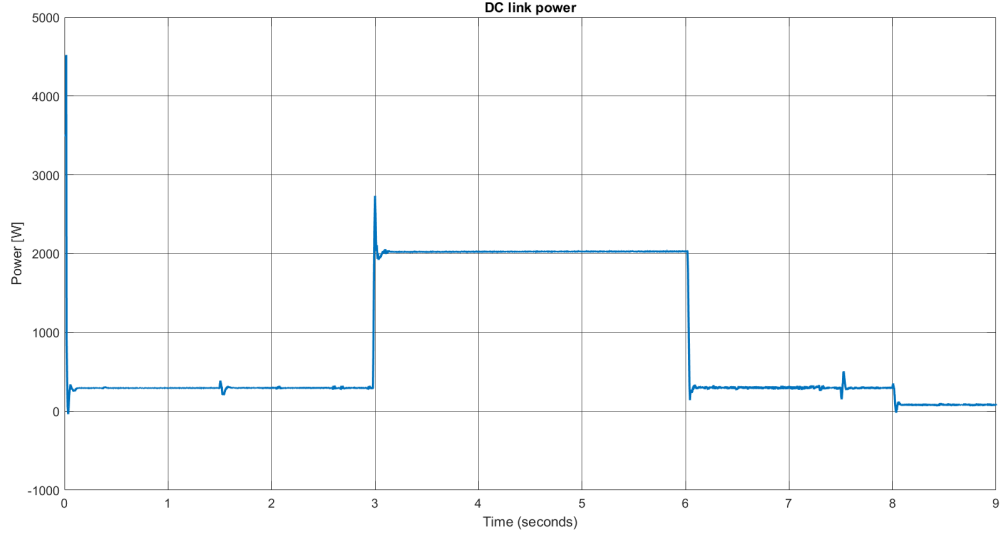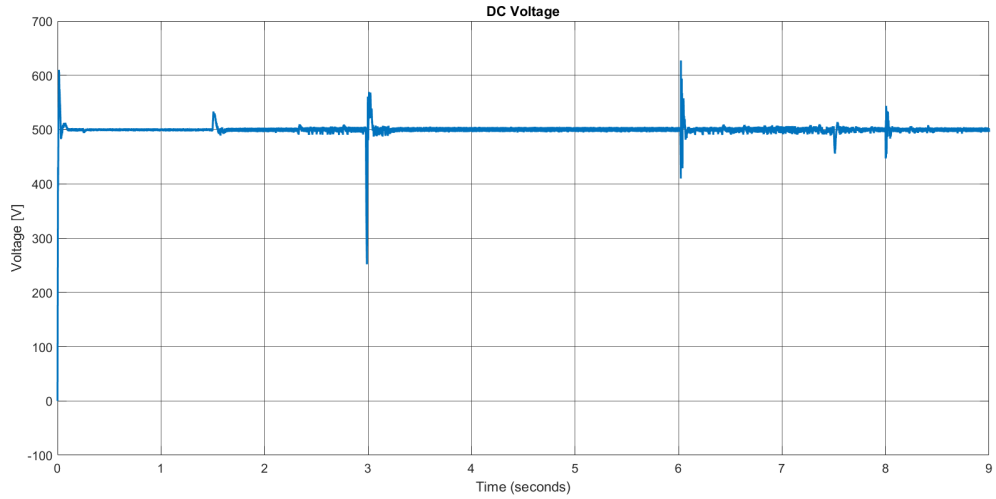
Figure 48: DC link power

Figure 49: DC link voltage.

The Figures(50,51,52) represents the load side results.

The d current component of the dq transformation(Figure 50) closely tracks the reference value established by the voltage-oriented control, even during sudden transitions. It stabilizes rapidly, ensuring a swift response to changes in the system.

As depicted in Figure 51, the power curve precisely aligns with the shape of the imposed power demand.
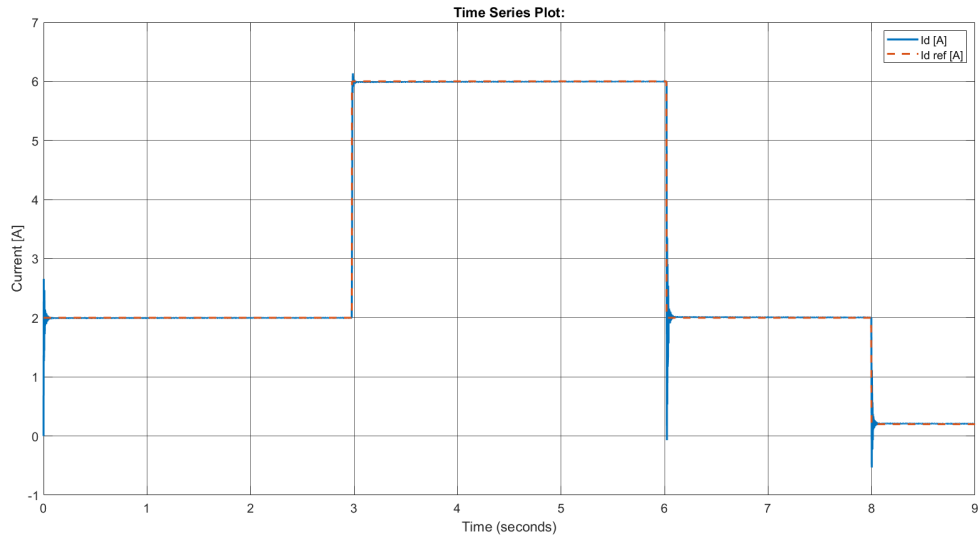
Figure 50: Id and reference current.

However, due to power being consumed by the battery for charging purposes, the exact value is not replicated. Additionally, the voltage and current closely track the values set by the Voltage control.
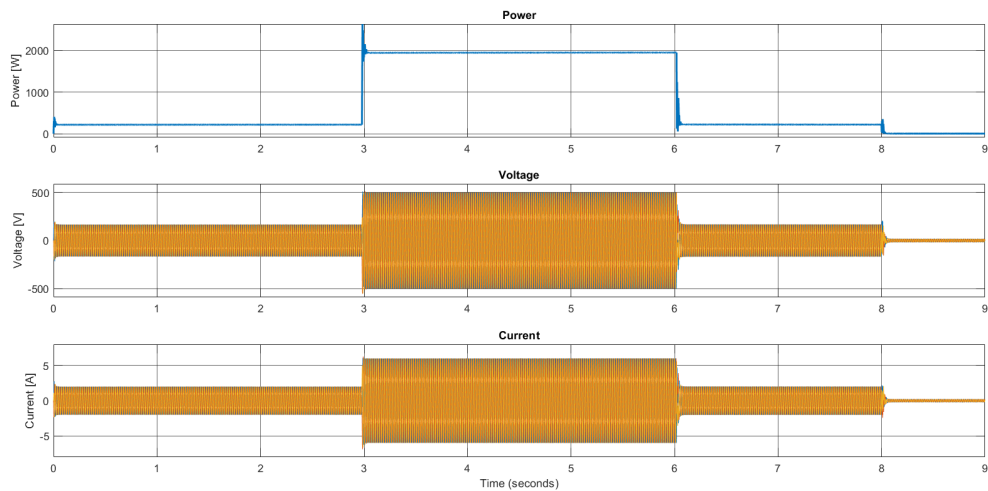

Figure 51: Load power, voltage and current.

Figure 52 Shows a zoomed in version of the load voltage and current, it is visible that the output is a smooth sinusoidal three-phase.
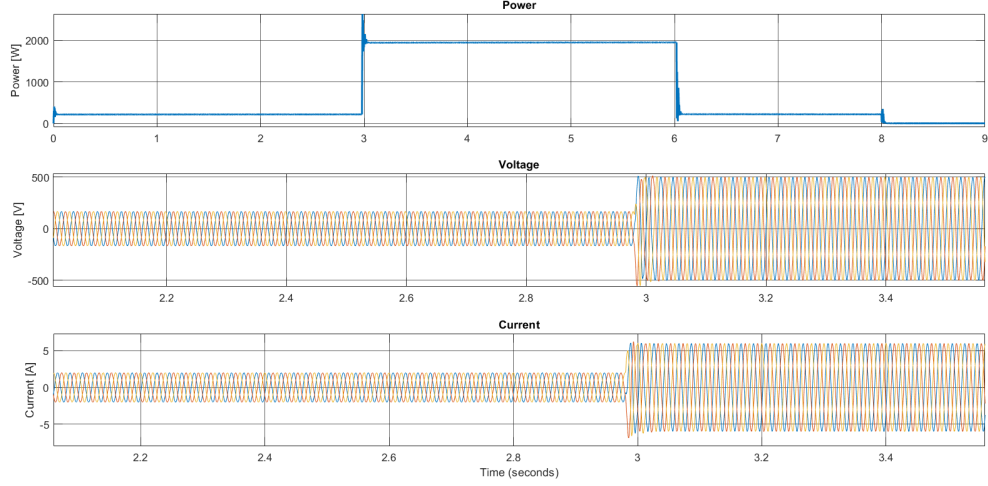
Figure 52: Load power, voltage and current.

4.5   Conclusion

Throughout this chapter, we have explored three simulation scenarios with varying parameters such as irradiances, power load demand, and State of Charge of the battery. Our aim was to evaluate the effectiveness of our energy management technique, which employs fuzzy logic control to switch different components of the system, ensuring a stable power delivery throughout each scenario.

Based on our findings, we can confidently conclude that our fuzzy logic controller adeptly adapts to changes within the system. It efficiently performs the necessary switches between the battery, diesel generator, and load shedding, effectively preventing the system from entering intermittent power mode.

General Conclusion

General Conclusion

The utilization of hybrid renewable energy systems, whether standalone or grid-connected, has emerged as a promising alternative. These systems have demonstrated their efficiency and environmental sustainability, offering a greener approach to meeting energy needs.

The implemented energy management system for this study is based on fuzzy logic, and its primary responsibility is to manage the switching of system components. The simulation tests showed that the use of fuzzy logic was effective specifically in transition between operation modes. This includes selecting the operation mode of the Energy Storage System, shedding secondary loads if necessary, or activating the backup diesel generator.

By employing these strategies, the system aims to ensure the effective utilization of the Hybrid Renewable Energy System (HRES) while maintaining a stable and uninterrupted power supply to consumers. The ultimate goal is to mitigate any potential electricity intermittence and deliver a seamless and consistent power experience.

As a future work we propose:

The use of advanced energy management methods using learning based techniques.

Design and perform in a deeper study while taking into consideration the cost from sizing to choosing cheaper materials to ensure a feasible system.

Perform a real-Time simulation and experimental implementation of the hybrid renewable energy system.

Appendix

A   Photovoltaic Panel

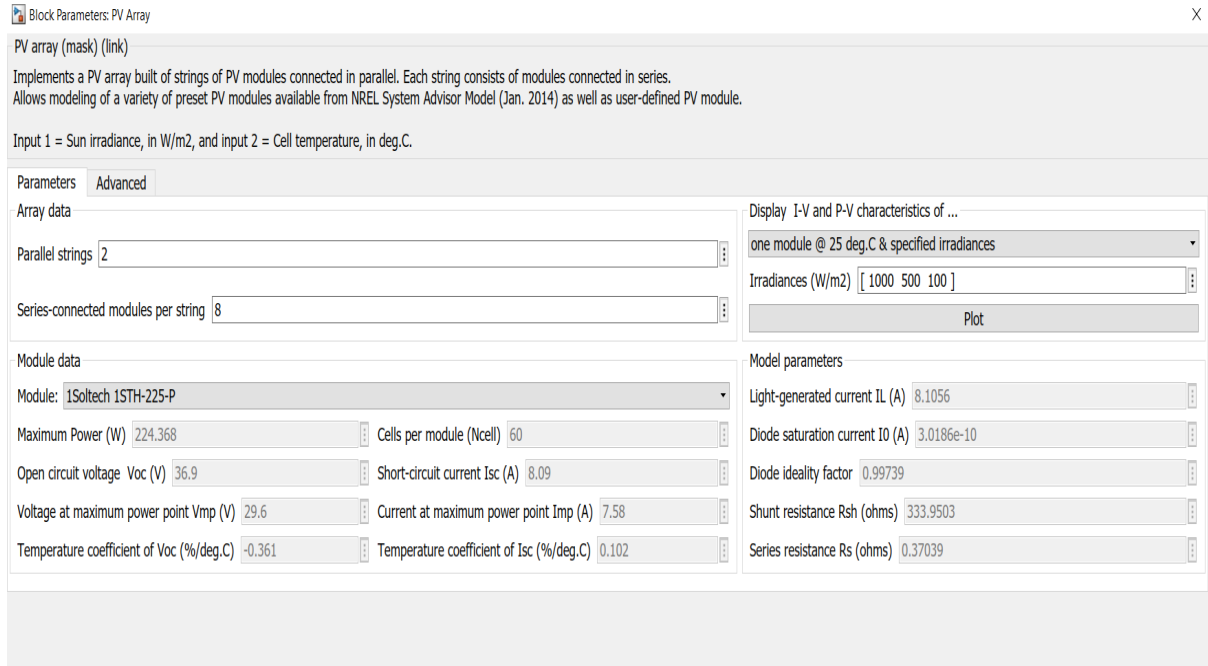The characteristics of the pv panel is shown in Figure 53

Figure 53: PV characteristics.
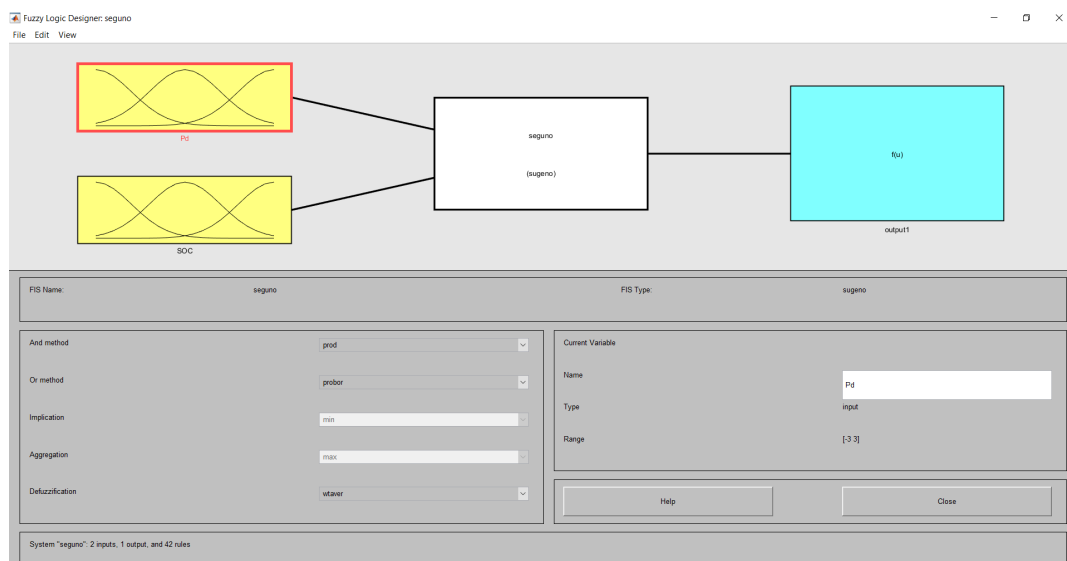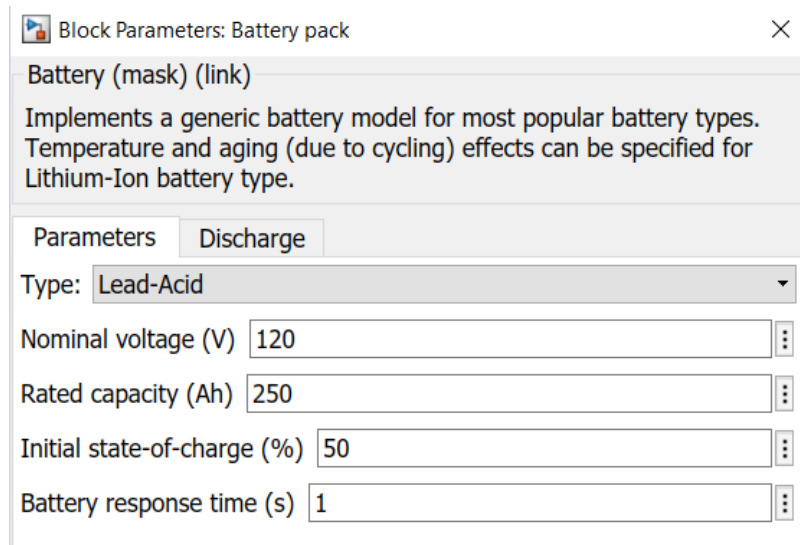
B   Fuzzy logic

Figure 54: Fuzzy logic control.

Figure 54 illustrates the configuration of the fuzzy inference system utilized in the energy management system. It is noteworthy that the employed technique follows the Takagi-Sugeno method. Additionally, the defuzzification method employed in this system is the weighted average (wtaver).

C Battery pack

Figure below illustrates battery pack characteristics used in the proposed system(Figure 55)

Figure 55: Battery pack charachteristics.

D PMSG Characteristics

Table 4.1 shows the parameters of PMSG used in the proposed system

Table 4.1: Technical Data of PMSG

Parameter	Value
Rated Output Power	4 kW
Rated Speed (rpm)	250
Frequency (Hz)	50
Number of Poles	24
Number of Phases	3
Rated Voltage (V)	400
Rated Power Factor	0.95

Bibliography

[1] JF Manwell et al. Hybrid energy systems. *Encyclopedia of energy*, 3(2004):215–229, 2004.

[2] Deepak Paramashivan Kaundinya, Palit Balachandra, and Nijavalli H Ravindranath. Grid-connected versus stand-alone energy systems for decentralized power—a review of literature. *Renewable and sustainable energy reviews*, 13(8):2041–2050, 2009.

[3] Energy Informative. Grid tied, off-grid and hybrid solar systems, 2019.

[4] JJ Ding and JS Buckeridge. Design considerations for a sustainable hybrid energy system. *Transactions of the Institution of Professional Engineers New Zealand: Electrical/Mechanical/Chemical Engineering Section*, 27(1):1–5, 2000.

[5] Obeida Farhat, Mahmoud Khaled, Jalal Faraj, Farouk Hachem, Rani Taher, and Cathy Castelain. A short recent review on hybrid energy systems: critical analysis and recommendations. *Energy Reports*, 8:792–802, 2022.

[6] Mohammad Reza Maghami and Arthur Guseni Oliver Mutambara. Challenges associated with hybrid energy systems: An artificial intelligence solution. *Energy Reports*, 9:924–940, 2023.

[7] Rodolfo Dufo-López, Tomás Cortés-Arcos, Jesús Sergio Artal-Sevil, and José L Bernal-Agustín. Comparison of lead-acid and li-ion batteries lifetime prediction models in stand-alone photovoltaic systems. *Applied Sciences*, 11(3):1099, 2021.

[8] Bhim Singh and Ram Niwas. Power quality improvement of pmsg-based dg set feeding three-phase loads. *IEEE Transactions on Industry Applications*, 52(1):466–471, 2015.

[9] Barney L Capehart, Wayne C Turner, and William J Kennedy. *Guide to energy management*. Crc Press, 2006.

[10] M. Sellali, A. Betka, and A. Djerdir. Power management improvement of hybrid energy storage system based on h control. *Mathematics and Computers in Simulation*, 167:478–494, 2020. INTERNATIONAL CONFERENCE on Emerging and Renewable Energy: Generation and Automation, held in Belfort, France on 4-6 July, 2017.

[11] Harpreetsingh Banvait, Sohel Anwar, and Yaobin Chen. A rule-based energy management strategy for plug-in hybrid electric vehicle (phev). In *2009 American control conference*, pages 3938–3943. IEEE, 2009.

[12] Nashat Jalil, Naim A Kheir, and Mutasim Salman. A rule-based energy management strategy for a series hybrid vehicle. In *Proceedings of the 1997 American Control Conference (Cat. No. 97CH36041)*, volume 1, pages 689–693. IEEE, 1997.

[13] Luis Santiago Azuara-Grande, Santiago Arnaltes, Jaime Alonso-Martinez, and Jose Luis Rodriguez-Amenedo. Ems for fuel saving in an isolated hybrid system (solar/diesel/battery). In *2020 IEEE International Conference on Environment and Electrical Engineering and 2020 IEEE Industrial and Commercial Power Systems Europe (EEEIC/I&CPS Europe)*, pages 1–4. IEEE, 2020.

[14] Sulochana Kengam and S Sreejith. An efficient energy management system for hybrid renewable energy sources. In *2019 Innovations in Power and Advanced Computing Technologies (i-PACT)*, volume 1, pages 1–6. IEEE, 2019.

[15] Dasheng Lee and Chin-Chi Cheng. Energy savings by energy management systems: A review. *Renewable and Sustainable Energy Reviews*, 56:760–777,

2016.

[16] Marcelo Gradella Villalva, Jonas Rafael Gazoli, and Ernesto Ruppert Filho. Comprehensive approach to modeling and simulation of photovoltaic arrays. *IEEE Transactions on power electronics*, 24(5):1198–1208, 2009.

[17] Mohammad H Moradi, SM Reza Tousi, Milad Nemati, N Saadat Basir, and N Shalavi. A robust hybrid method for maximum power point tracking in photovoltaic systems. *Solar Energy*, 94:266–276, 2013.

[18] Aymen Chaouachi, Rashad M Kamel, and Ken Nagasaka. A novel multi-model neuro-fuzzy-based mppt for three-phase grid-connected photovoltaic system. *Solar energy*, 84(12):2219–2229, 2010.

[19] Robert W Erickson. Dc–dc power converters. *Wiley encyclopedia of electrical and electronics engineering*, 2001.

[20] N Achaibou, M Haddadi, and A Malek. Modeling of lead acid batteries in pv systems. *Energy procedia*, 18:538–544, 2012.

[21] Clarence M Shepherd. Design of primary and secondary cells: Ii. an equation describing battery discharge. *Journal of the Electrochemical Society*, 112(7):657, 1965.

[22] Peng Zhang, Jun Liang, and Feng Zhang. An overview of different approaches for battery lifetime prediction. In *IOP Conference Series: Materials Science and Engineering*, volume 199, page 012134. IOP Publishing, 2017.

[23] Rachid Darbali-Zamora, Jimmy E Quiroz, Javier Hernández-Alvidrez, Jay Johnson, and Eduardo I Ortiz-Rivera. Viability assessment of a real-time simulation model for a residential dc microgrid network to compensate electricity disturbances in puerto rico. In *2018 IEEE ANDESCON*, pages 1–6. IEEE, 2018.

[24] Youness El Mourabit, Aziz Derouich, Abdelaziz El Ghzizal, Najib El Ouanjli,

and Othmane Zamzoum. Nonlinear backstepping control for pmsg wind tur-bine used on the real wind profile of the dakhla-morocco city. *International Transactions on Electrical Energy Systems*, 30(4):e12297, 2020.

[25] Ihab S Mohamed, Stefano Rovetta, Ton Duc Do, Tomislav Dragicević, and Ahmed A Zaki Diab. A neural-network-based model predictive control of three-phase inverter with an output *lc* filter. *IEEE Access*, 7:124737–124749, 2019.

[26] A Chouder, F Guijoan, and S Silvestre. Simulation of fuzzy-based mpp tracker and performance comparison with perturb & observe method. *Journal of Re-newable Energies*, 11(4):577–586, 2008.

[27] Shruti Sahu, Gayadhar Panda, and Satya Prakash Yadav. Dynamic modelling and control of pmsg based stand-alone wind energy conversion system. In *2018 Recent Advances on Engineering, Technology and Computational Sciences (RAETCS)*, pages 1–6. IEEE, 2018.

[28] Zhou Feng, Zhou Jingjing, Xiao Ji, Cheng Yingying, Feng Ling, Li Zhe, Du Jie, and Zhang Jiaming. Energy management strategy of microgrid based on fuzzy control. In *2018 2nd IEEE Advanced Information Management, Communicates, Electronic and Automation Control Conference (IMCEC)*, pages 1–1670. IEEE, 2018.

[29] PWM Cichowlas. *Rectifier with Active Filtering, Warsaw University of Tech-nology*. PhD thesis, Ph. D. Thesis, Warsaw, Poland, 2004.

[30] S Lechat Sanjuan. Voltage oriented control of three-phase boost pwm convert-ers. *Chalmers University of Technology*, 2010.